THE JOURNAL OF PHYSICAL CHEMISTRY C

Article

pubs.acs.org/JPCC

Vibrational Excitation of H_2 Scattering from Cu(111): Effects of Surface Temperature and of Allowing Energy Exchange with the Surface

Geert-Jan Kroes,*[,†] J. I. Juaristi,[‡,§,∥] and M. Alducin[§,∥]

[†]Leiden Institute of Chemistry, Gorlaeus Laboratories, Leiden University, P.O. Box 9502, 2300 RA Leiden, The Netherlands

[‡]Departamento de Física de Materiales, Facultad de Químicas, Universidad del País Vasco/Euskal Herriko Unibertsitatea (UPV/EHU), Apartado 1072, 20080 Donostia-San Sebastián, Spain

[§]Centro de Física de Materiales (CFM/MPC), Consejo Superior de Investigaciones Científicas (CSIC)-UPV/EHU, Paseo Manuel de Lardizabal 5, 20018 Donostia-San Sebastián, Spain

[∥]Donostia International Physics Center (DIPC), Paseo Manuel de Lardizabal 4, 20018 Donostia-San Sebastián, Spain

ABSTRACT: In scattering of H_2 from Cu(111), vibrational excitation has so far defied an accurate theoretical description. To expose the causes of the large discrepancies with experiment, we investigate how the feature due to vibrational excitation (the "gain peak") in the simulated time-of-flight spectrum of (v = 1, j = 3) H_2 scattering from Cu(111) depends on the surface temperature (T_s) and the possibility of energy exchange with surface phonons and electron−hole pairs (ehp's). Quasi-classical dynamics calculations are performed on the basis of accurate semiempirical density functionals for the interaction with H_2 + Cu(111). The methods used include the quasi-classical trajectory method within the Born−Oppenheimer static surface model, the generalized Langevin oscillator (GLO) method incorporating energy transfer to surface phonons, the GLO + friction (GLO+F) method also incorporating energy exchange with ehp's, and ab initio molecular dynamics with electronic friction (AIMDEF). Of the quasi-classical methods tested, comparison with AIMDEF suggests that the GLO+F method is accurate enough to describe vibrational excitation as measured in the experiments. The GLO+F calculations also suggest that the promoting effect of raising T_s on the measured vibrational excitation is due to an electronically nonadiabatic mechanism. However, by itself, enabling energy exchange with the surface by modeling surface phonons and ehp's leads to reduced vibrational excitation, further decreasing the agreement with experiment. The simulated gain peak is quite sensitive to energy shifts in calculated vibrational excitation probabilities and to shifts in a specific experimental parameter (the chopper opening time). While the GLO+F calculations allow important qualitative conclusions, comparison to quantum dynamics results suggests that, with the quasi-classical way of describing nuclear motion and the present box quantization method for assigning the final vibrational state, the gain peak is not yet described with quantitative accuracy. Ways in which this problem might be resolved in the future are discussed.

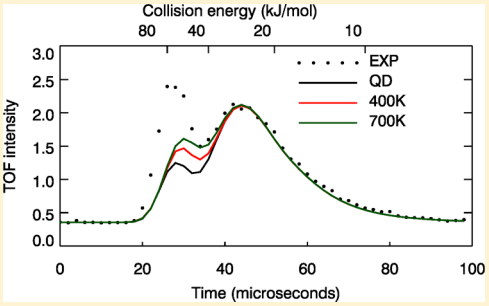

1. INTRODUCTION

In scattering of a diatomic molecule from a metal surface, vibrational excitation may be intimately linked to the molecule's dissociative chemisorption, as bond stretching is involved in both cases. Given the importance of elementary molecule−metal surface reactions to heterogeneous catalysis[1,2] and the observation that vibrationally inelastic scattering can probe the barrier region of reactive potential energy surfaces (PESs),[3−6] it is not surprising that vibrationally inelastic scattering of molecules from metal surfaces has become a subject of intense study. Systems that have been studied experimentally include H_2 + Cu(111),[3,4,7] H_2 + Cu(100),[8,9] NO + Au(111),[10,11] NO + Ag(111),[12] N_2 + Pt(111),[13] HCl + Au(111),[14] and CO + Au(111).[15]

There is considerable evidence that vibrationally inelastic scattering of molecules other than H_2 from metal surfaces is governed by an electronically nonadiabatic mechanism.[10−15] However, the H_2 + Cu(111) system has often been viewed as a system in which vibrational excitation happens in a mostly adiabatic mechanism, in competition with dissociative chemisorption and resulting from the stretching of the molecule as it approaches its transition state.[3,4,16] Features have been identified in the PESs for H_2 interacting with low-index Cu surfaces that are thought to promote vibrational excitation in an electronically adiabatic manner.[5,6,17] These considerations would seem to make vibrational excitation in H_2 + Cu systems a phenomenon that should be straightforward to model and understand, but as will now be discussed, this is not true.

Vibrationally inelastic scattering of H_2 from copper surfaces has been studied experimentally for H_2 + Cu(111)[3,4,7] and H_2 +

Received: February 3, 2017
Revised: May 23, 2017
Published: June 5, 2017

DOI: 10.1021/acs.jpcc.7b01096
J. Phys. Chem. C 2017, 121, 13617−13633

Cu(100).[8,9] In a detailed study on H_2 + Cu(111),[7] on which we will focus, a high-energy molecular beam was scattered from Cu(111) at an incidence angle that was slightly off-normal (θ_i = 15°), with the $[1\bar{2}1]$ azimuth selected as the incidence plane. The amount of H_2 molecules scattered to the (v = 1, j = 3) state (v is the quantum number for vibration and j the quantum number for rotation) was determined in a time-resolved manner, using resonance enhanced multiphoton ionization (REMPI) and time-of-flight (TOF) techniques. With the setup that was used, vibrational excitation from several (v = 0, j) states to (v = 1, j = 3) is evident from a peak occurring at short times in the time-of-flight spectrum (see Figure 1). By reference

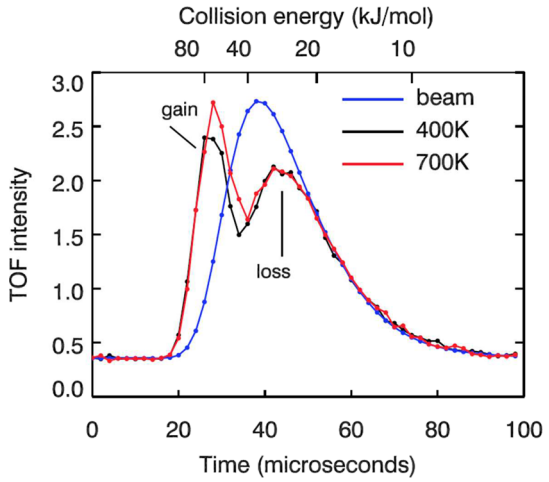

Figure 1. Time-of-flight spectrum of (v = 1, j = 3) H_2 scattering from Cu(111) at a surface temperature (T_s) of 400 K (black dots) or 700 K (red dots) or in a freely traveling molecular beam (blue dots) at a position corresponding to the same flight length as traversed by H_2 in the scattering experiment. In all cases the data points were connected by lines, which merely serve to guide the eye. The data were taken from refs 7 and 16.

to the TOF signal of a freely moving H_2 beam, Rettner et al. called this peak the "gain peak".[7] At longer times another broad peak was evident (Figure 1), which reflects rotationally inelastic scattering within v = 1 as well as loss of (v = 1, j = 3) H_2 due to dissociative chemisorption and vibrational de-excitation. This peak was therefore called the "loss peak".[7] Using an equation similar to the one we will be using below in attempts to reproduce this experiment, Rettner et al. were able to extract quantitative information on vibrational excitation on the assumption that j should be conserved in the vibrational excitation process (i.e., vibrational excitation probabilities $P(v = 0, j = 3 \rightarrow v = 1, j = 3)$).[7] Theoretical work later indicated that this assumption is not justified, because j is not conserved in vibrational excitation and because the total vibrational excitation probability to v = 1 depends rather strongly on the initial value of j in the initial (v = 0, j) state of H_2.[18] Finally, experiments performed for surface temperatures (T_s) of 400 and 700 K suggested that raising T_s weakly promotes vibrational excitation[7] (see also Figure 1), which has been attributed to a mechanism involving surface phonons.[16]

Prior to 2009, attempts to describe vibrationally inelastic scattering of H_2 from Cu(111) were severely hampered by the accuracy in the potential energy surfaces (PESs) used in the dynamics calculations. By this, we mean that discrepancies between calculations and experimental observations could always be blamed on inaccuracies in the PES used in the calculations. This changed to a large extent when in 2009 a chemically accurate PES became available for H_2 + Cu(111), from a semiempirical implementation of density functional theory (DFT).[19] With this PES, sticking probabilities of H_2 and D_2 on Cu(111),[19] the influence of the initial vibrational and rotational states of H_2[19] and D_2[20] on reaction on Cu(111), and rotational excitation of H_2 scattering from Cu(111)[19] could all be described with chemical accuracy. The PES also allowed an accurate description of the rotational quadrupole alignment parameter of D_2 desorbing from Cu(111) in two rovibrational states.[21] The good performance of the PES for a variety of reactive scattering experiments (in addition to rotationally inelastic scattering) suggests the PES (or the accompanying density functional) should also be good for studying vibrationally inelastic scattering, which occurs in competition with reaction and in the same energy regime.[7] Nevertheless, quantum dynamics (QD) calculations carried out within the Born−Oppenheimer static surface approximation (BOSS model) and using this PES underestimated the gain peak in the TOF spectrum of Figure 1 by about a factor of 3. By this, we mean that the calculated vibrational excitation probabilities had to be multiplied by a factor of 3 to reproduce the TOF spectrum.[16,22]

Further analysis suggested that this failure should be primarily due to the failure of the dynamical model (i.e., the BOSS model) rather than to the PES used.[16] Specifically, the analysis showed that if seemingly plausible assumptions were made about how vibrational excitation should change from the hypothetical T_s effectively used in the theory (0 K) to its experimental value (400 K), and about the size of energy loss to the surface, the discrepancy between theory and experiment could be reduced to a factor of 2.[16] It was suggested that the absence of phonons in the dynamical model should be primarily responsible for the discrepancy between theory and experiment.[16] Another suggestion was to examine this further with ab initio molecular dynamics (AIMD) calculations, if possible with the method extended in such a way that electron−hole pair (ehp) excitation could also be modeled with an electronic friction approach to examine its role. The expectation was formulated[16] that the quasi-classical treatment of nuclear motion should not represent a severe limitation, as the quasi-classical trajectory (QCT) method should already be reasonably accurate for describing vibrational excitation at the collision energy (80 kJ/mol)[23] at which the contribution of vibrational excitation to the gain peak in Figure 1 peaks.

Meanwhile, it has become possible to perform AIMD calculations with an electronic friction description of ehp excitation (AIMD with electronic friction, or AIMDEF).[24−27] However, the method is still quite expensive, especially if the goal is to obtain scattering probabilities with high statistical accuracy for a large range of incidence energies and initial states, as required for the accurate simulation of the measured TOF spectrum[7] (the gain peak in Figure 1). Here, we will use the AIMDEF method to benchmark a computationally much cheaper to use method incorporating the effects of phonons and electronic friction, i.e., a generalized Langevin oscillator method incorporating electronic friction (GLO+F).[28,29] We will show that, compared to AIMDEF, the GLO+F method accurately describes vibrational excitation of H_2 up to and including the incidence energy (E_i) most relevant to the simulation of the experiment, while exhibiting still reasonable accuracy for higher E_i.

DOI: 10.1021/acs.jpcc.7b01096
J. Phys. Chem. C 2017, 121, 13617−13633

The goals of the present work are as follows: We will explore whether the QCT method used in GLO, GLO+F, and AIMDEF calculations is capable of yielding quantitatively accurate results for the simulated TOF spectrum exhibiting vibrationally inelastic scattering, through comparison with quantum simulations. Next, we will use the QCT and the GLO+F methods to explore whether previous speculation of how vibrational excitation probabilities should depend on the incidence angle[16] was correct. This is useful knowledge as the need for performing quantum calculations for off-normal incidence would make a QD approach much more computationally expensive. Next, GLO and GLO+F calculations are used to explore how introducing surface phonon motion and ehp excitation into the dynamical model affects calculated vibrational excitation probabilities and whether their inclusion improves the agreement between the simulated and experimental TOF spectra, as speculated earlier.[16] We will also investigate whether the promotion of vibrational excitation through increased surface temperature[7] is due to heating the surface phonons, as assumed earlier,[16] or to heating the metal electrons. The calculations will reveal that the measured TOF spectrum is highly sensitive to how quickly the vibrational excitation probabilities rise above their threshold. We will therefore also perform some simulations to establish how shifting quantum dynamically calculated vibrational excitation probabilities along the energy axis, and uncertainties in the origin of time in the experiments (i.e., the beam chopper opening time), affect the computed TOF spectrum and its comparison to experiment.

This paper is set up as follows: Section 2 describes the methods used, their implementation, and numerical details. Specifically, section 2.1 describes how to simulate the experimental TOF spectrum exhibiting vibrational excitation. Sections 2.2, 2.3, 2.4, and 2.5 describe the QCT, the GLO, the GLO+F, and the AIMDEF methods used. Section 2.6 discusses how the molecule−surface interaction and, from these, the forces are obtained in the present work. Section 2.7 discusses several details of the implementation of the methods, such as operational definitions of scattering probabilities, the generation of initial conditions, the running of trajectories, and numerical details. Section 3.1 presents the results of benchmarking the GLO+F method against the AIMDEF method. Section 3.2 presents QCT, GLO, and GLO+F calculations for normal incidence, also benchmarking the QCT method against QD. Section 3.3 investigates the effect of the incidence angle. Like the preceding section, this section also discusses the effects of introducing phonons and electronically nonadiabatic effects in the dynamics calculations, and which of these effects promote vibrational excitation if the surface temperature is raised. Section 3.4 presents the results on how shifting vibrational excitation probabilities along the energy axis, and the time-origin in the experiments, affect the simulated TOF spectrum. Section 3.5 discusses how the theoretical description of vibrationally inelastic scattering of H_2 from Cu(111) (or from metal surfaces in general) might be improved in the future. Conclusions are presented in section 4.

2. METHOD

2.1. Modeling the Experiment. In the experiments we simulate (see Figure 1 of ref 7), a chopped molecular beam of H_2 molecules travels toward a Cu(111) crystal and is scattered from it. The incident beam makes a polar angle $\theta_i = 15°$ with the surface normal, and the incidence is along the $[1\bar{2}1]$ azimuth.[7] The amount of molecules scattered from the surface in the $(v' = 1, j' = 3)$ state is measured in a time-resolved manner with REMPI and can be described according to[7,16]

$$S(t) = c + N\left\{\left(\frac{v_i}{v_0}\right)^4 \exp\left[-\left(\frac{v_i - v_0}{\alpha(v_i)}\right)^2\right] P(v = v', j = j' \rightarrow v' = 1, j' = 3) + x_t\left[\sum_{vj,v'j'\neq vj}\left(\frac{{v_i}^3}{v_s {v_0}^4}\right)\left(\frac{1}{x_i {v_i}^{-2} + x_s v_i {v_s}^{-3}}\right) \exp\left[-\left(\frac{(v_i - v_0)}{\alpha(v_i)}\right)^2\right] w_{vj} P(v, j \rightarrow v' = 1, j' = 3)\right]\right\} \quad (1)$$

In eq 1, t measures the time from the opening of the chopper and v_i and v_s are the velocities of the incident and scattered molecules, respectively, with both depending on the initial (v, j) state of H_2 and t through energy conservation, as described in ref 7. However, in some cases we take into account that the scattered molecule incurs a loss of a fraction f_l of the kinetic energy that would be available to it if it were to scatter from a static surface in an electronically adiabatic manner:

$$1/2 m {v_s}^2 = (1 - f_l)(E_i - [E_{v=1,j=3} - E_{vj}]) \quad (2)$$

Here, m is the mass of H_2, E_i its incident translational energy, and E_{vj} its internal rovibrational energy depending on v and j. Furthermore, v_0 is the stream velocity of the molecular beam (4115 m/s), and $\alpha(v_i)$ a width parameter that can take on one of two values depending on v_i (1358 or 2379 m/s for $v_i < v_0$ or $v_i > v_0$, respectively).[7] Also, N is a normalization factor, and c defines an offset; x_i and x_s define the distance traveled by the incident and scattered molecules, and x_t defines their sum (values are given in ref 7). The Boltzmann population of the initial (v, j) state in the beam divided by the Boltzmann population of the initial $(v = 1, j = 3)$ state in the beam is given by the weight factor w_{vj}. For the nearly effusive beam used in the experiments, these populations may be calculated assuming that both the rotational and the vibrational temperatures were equal to the nozzle temperature T_n of 2000 K.[7]

The use of a nearly effusive beam with a high value of T_n (i.e., with a broad energy distribution) in combination with the chopper and the detecting laser allowed the experimentalists to obtain vibrational excitation probabilities for very high E_i, which are not accessible in ordinary supersonic molecular beam experiments on H_2. Although, at the time of writing, the experiments were done almost 25 years ago, they are quite well documented and yet to be surpassed in accuracy and information content when it comes to experiments on vibrational excitation of H_2 scattering from metal surfaces.

For the simulation of the TOF signal described by eq 1, the crucial inputs from dynamics calculations are the state-to-state probabilities $P(v, j \rightarrow v' = 1, j' = 3)$ and the fractional energy losses f_l (eq 2), which may be taken to be dependent on v and j. Upon scattering, fractional energy losses may occur that reflect energy loss to phonons (in GLO, GLO+F, and AIMDEF calculations), to ehp's (in GLO+F and AIMDEF calculations), and to translational motion perpendicular to the scattering plane (in all calculations performed for off-normal incidence).

DOI: 10.1021/acs.jpcc.7b01096
J. Phys. Chem. C 2017, 121, 13617−13633

2.2. Quasi-Classical Trajectory (QCT) Method. In the calculations with the QCT method,[30] the momenta and positions of the H atoms labeled by i and j are evolved according to Hamilton's equations of motion

$$\frac{d\mathbf{p}_i}{dt} = -\nabla_i V(\mathbf{r}_i, \mathbf{r}_j) \tag{3}$$

$$\frac{d\mathbf{r}_i}{dt} = \mathbf{v}_i \tag{4}$$

In eq 3, $V(\mathbf{r}_i, \mathbf{r}_j)$ is a six-dimensional potential energy surface describing the interaction of the two H atoms at positions $\mathbf{r}_i$ and $\mathbf{r}_j$ with one another and with the static Cu(111) surface, and in eq 4, the velocities of the atoms are represented by $\mathbf{v}_i$. The QCT method differs from the ordinary classical trajectory method in that in the QCT method zero-point vibrational energy (possibly added to extra vibrational energy if the molecule is vibrationally excited initially) is always imparted to the molecule at the start of the trajectories.

2.3. Generalized Langevin Oscillator (GLO) Method. In the GLO method,[31−33] eq 3 is rewritten as

$$\frac{d\mathbf{p}_i}{dt} = -\nabla_i V(\mathbf{r}_i - \mathbf{r}_s, \mathbf{r}_j - \mathbf{r}_s) \tag{5}$$

In eq 5, $\mathbf{r}_s$ is the position of the surface atom nearest to H_2, which is taken to move as a three-dimensional harmonic oscillator with mass m_s (here taken as the mass of a surface Cu atom). The momentum of the surface atom obeys

$$\frac{d\mathbf{p}_s}{dt} = -\nabla_s V(\mathbf{r}_i - \mathbf{r}_s, \mathbf{r}_j - \mathbf{r}_s) - m_s\boldsymbol{\Omega}^2\mathbf{r}_s + m_s\boldsymbol{\Lambda}_{gs}\mathbf{r}_g \tag{6}$$

where $\boldsymbol{\Omega}^2$ is the diagonal 3 × 3 frequency matrix associated with the surface harmonic oscillator and $\boldsymbol{\Lambda}_{gs}$ is a diagonal 3 × 3 matrix that couples the motion of the surface to a ghost oscillator with position $\mathbf{r}_g$. In turn, the momentum of the ghost oscillator is given by

$$\frac{d\mathbf{p}_g}{dt} = -m_s\boldsymbol{\Omega}^2\mathbf{r}_g + m_s\boldsymbol{\Lambda}_{gs}\mathbf{r}_s - \eta_{ph}\frac{d\mathbf{r}_g}{dt} + \mathbf{R}^{ph}(T_s) \tag{7}$$

The third term on the right-hand side (rhs) of eq 7 models energy dissipation from the surface to the bulk of copper through a friction coefficient η_{ph}, which is computed from

$$\eta_{ph} = m_s\pi\omega_D/6 \tag{8}$$

where ω_D is the Debye frequency of the solid.[32] The randomly fluctuating force $\mathbf{R}^{ph}$ is modeled as Gaussian white noise with variance[34]

$$\mathrm{Var}[\mathbf{R}^{ph}(T_s)] = \frac{2k_B T_s \eta_{ph}}{\Delta t} \tag{9}$$

In eq 9, Δt is the time step used in the integration of the equations of motion and k_B is the Boltzmann constant. The linking of the randomly fluctuating force with the phonon friction coefficient ensures that the fluctuation−dissipation theorem is obeyed,[34] so that thermal equilibrium can be restored after the direct scattering event (i.e., in the present case of H_2 + Cu(111)). The elements of the diagonal matrix $\boldsymbol{\Omega}^2$ are equal to $2\omega_i^2$, and the elements of the diagonal coupling matrix $\boldsymbol{\Lambda}_{gs}$ are equal to ω_i^2, with ω_i being the surface phonon frequencies ($i = x, y, z$).

2.4. Generalized Langevin Oscillator with Electronic Friction (GLO+F) Method. In the GLO+F method,[28,34] eq 3 is extended further to

$$\frac{d\mathbf{p}_i}{dt} = -\nabla_i V(\mathbf{r}_i - \mathbf{r}_s, \mathbf{r}_j - \mathbf{r}_s) - \eta_{el,i}(\mathbf{r}_i - \mathbf{r}_s)\frac{d\mathbf{r}_i}{dt} + \mathbf{R}^i_{el}[T_s, \eta_{el,i}(\mathbf{r}_i - \mathbf{r}_s)] \qquad i \neq j \tag{10}$$

In eq 10, the effect of energy transfer involving ehp's is modeled with molecular dynamics with electronic friction (MDEF)[35] using the local density friction approximation (LDFA)[36] in the independent atom approximation (IAA).[36] The friction coefficients used in the LDFA have been successfully applied to calculate the stopping power of atoms and ions by metal solids and surfaces[37−40] and in the modeling of scattering of H atoms from Au surfaces.[41] When using the IAA to apply the method to molecules, the assumption is made that the electronic friction is independent of the electronic structure of the molecule, so that electronic friction forces can be specified through atomic friction coefficients $\eta_{el,i}$, as done in eq 10. In the LDFA, the atomic electronic friction coefficients depend on the electronic density of the bare metal surface at the position of the atom relative to the surface.[36] The LDFA-IAA method has now been used to study the effect of electronic excitations on the dynamics of molecules scattering from metal surfaces in several applications,[28,29,36,42,43] including the H_2 + Cu(111) system.[44] In eq 10, the randomly fluctuating force $\mathbf{R}^i_{el}$ represents the nonadiabatic scattering of thermal surface electrons from the molecule. To ultimately enable descriptions in which the molecule becomes equilibrated to the surface, the fluctuation−dissipation theorem is taken into account[45] by modeling this force as Gaussian white noise with variance[34]

$$\mathrm{Var}[\mathbf{R}^i_{el}(T_s)] = \frac{2k_B T_s \eta_{el,i}}{\Delta t} \tag{11}$$

2.5. Ab Initio Molecular Dynamics with Electronic Friction (AIMDEF) Method. In the calculations with the AIMDEF method,[24−26] essentially quasi-classical calculations are carried out for the nuclear dynamics, with the forces calculated on the fly from DFT. Of course, we also model ehp excitation, by adding electronic friction forces and a randomly fluctuating force (second and third terms on the rhs of eq 10) to the adiabatic forces on the H atoms in the simulations. The motion of not just the impinging H_2 molecule, but also the Cu atoms in the upper layers of the Cu(111) slab is simulated. The Cu(111) slab is thermalized prior to the scattering calculations at the experimental T_s. Since the scattering and reaction of H_2 on Cu(111) occur in a direct manner (without the molecule performing several bounces on the surface), there is no need to thermalize the atoms in the layers in which they are allowed to move while the collision proceeds. Therefore, we simply have one layer of stationary Cu atoms at the bottom of the slab in the simulations we carry out, and the GLO formalism is not applied to the motion of these atoms.

2.6. Molecule−Surface Interaction. In the QCT, GLO, and GLO+F calculations, the original specific reaction parameter (SRP) PES for H_2 + Cu(111) was used. The SRP functional used effectively to generate the PES[19,22] is a weighted average of the revised Perdew−Burke−Ernzerhof (RPBE) functional[46] (mixing coefficient 0.43) and the Perdew−Wang 1991 (PW91) functional[47] (mixing coefficient 0.57). Further details of its calculation can be found in refs 19

DOI: 10.1021/acs.jpcc.7b01096
J. Phys. Chem. C 2017, 121, 13617−13633

and 22, and elbow plots of two-dimensional cuts through the PES are shown in Figure S1 of ref 19. The SRP barrier geometry and height are provided in Table 1 for two

Table 1. SRP Minimum-Barrier Geometry and the SRP and SRP48 Values of the Molecule−Surface Interaction Energy E at These Geometries[a]

geometry	d_b (bohr)	Z_b (bohr)	E (eV), SRP	E (eV), SRP48
bridge-to-hollow	1.95	2.20	0.628	0.628
top-to-bridge	2.64	2.62	0.891	0.876

[a]In all cases, H_2 is parallel to the surface. d_b is the H−H distance and Z_b the molecule−surface distance at the barrier.

geometries, i.e., the minimum-barrier geometry in which H_2 impacts on a bridge site, with the H atoms moving to hollow sites (bth), and a geometry in which H_2 impacts on a top site, with the H atoms moving to bridge sites (ttb). The first geometry is most relevant for reaction at low E_i, while the second geometry is thought to be most important to vibrational excitation, as the features of the elbow cut are thought to be conducive to vibrationally inelastic scattering (reaction path with large curvature in front of an especially late barrier;[5,6,17] see also Figure S1E of ref 19).

For reasons related to the need for being able to work with a variable (i.e., T_s-dependent) lattice constant, which are discussed in detail in ref 21 and its accompanying Supporting Information, the SRP functional had to be reparametrized to enable AIMD (and, here, AIMDEF) calculations.[21] With the reparametrized (i.e., SRP48) functional (which is a weighted average of the RPBE functional[46] (mixing coefficient 0.48) and the PBE functional[48] (mixing coefficient 0.52)), the molecule−surface interaction at the SRP minimum-barrier bth geometry is reproduced to within better than 1 meV, while the molecule−surface interaction at the SRP ttb barrier geometry is reproduced to within 15 meV (see ref 21 and Table 1). Therefore, the use of a density functional in the AIMDEF simulations somewhat different from the one implicit in the use of the SRP PES in the QCT, GLO, and GLO+F calculations should, taken by itself, only lead to small discrepancies between the calculated vibrational excitation probabilities.

2.7. Numerical Details and Implementation. *2.7.1. Operational Definition of Reaction and of Rovibrationally Inelastic Scattering.* In all calculations a similar operational definition is used for reaction and for rovibrationally inelastic scattering. Reaction is defined to occur once the H−H distance in a trajectory becomes larger than 1.6 Å in the AIMDEF calculations (2.2 Å in all other calculations). Scattering is defined to occur once the molecule−surface distance becomes larger than 6.1 Å, with the velocity of the molecule pointing away from the surface in the AIMDEF calculations (9 Å in all other calculations).

The assignment of the final rovibrational state is done as follows: The classical analogue of the rotational quantum number is computed as

$$j_q = -1/2 + \sqrt{1/4 + j_c^2} \tag{12}$$

where j_c is the classical rotational angular momentum. Next, the rotational quantum state j is assigned by binning j_q to the nearest odd value of j, keeping in mind the conservation of parity in H_2 and our interest in scattering to an odd j state within $v = 1$ (i.e., ($v = 1$, $j = 3$);[7] see also section 2.1). The vibrational state v is then assigned by computing the classical rovibrational energy of the molecule and comparing it to the quantum mechanical vibrational energies within the j ladder and assigning v to describe the (v, j) state with the nearest rovibrational energy in that ladder. Probabilities (whether for reaction or rovibrationally inelastic scattering) are simply computed by dividing the number of trajectories resulting in the outcome of interest by the total number of trajectories. In the AIMDEF calculations, a total of 1100 trajectories were run for each E_i. Much larger numbers of trajectories were computed in the QCT, GLO, and GLO+F calculations, i.e., 200000 trajectories for each v, j state at each E_i.

2.7.2. Initial Conditions. H_2 was initialized with is center of mass 6 Å away from the surface in the AIMDEF calculations (9 Å in all other calculations), with a velocity directed toward the surface according to the E_i simulated. Depending on the simulation, either the incidence direction was normal to the surface or the incidence angles were taken equal to the experimental values (see below). A Monte Carlo integration was performed over randomly selected impact points on the surface and initial orientation angles and directions of rotational velocities, in accordance with the initial value of j and the initial magnetic rotational quantum number m_j (the projection of j on the surface normal) as described in, for instance, ref 49. In the AIMDEF calculations, a uniform sampling of m_j was performed by running equal numbers of trajectories for $-j \le m_j \le j$. In all other calculations, instead a random sampling was performed of the orientation of the classical angular momentum for each j. Initial values of the H−H distance d and its conjugate momentum were selected by performing a uniform sampling in time of these values along a one-dimensional quasi-classical trajectory run for isolated H_2 for the quantum mechanical energy computed for the relevant initial (v, j) state with the Fourier-grid Hamiltonian method.[50]

In the GLO and GLO+F calculations, the initial position of the surface atom, $\mathbf{r}_s$, and its conjugate momenta are sampled through a conventional Monte Carlo procedure in such a way that they correspond to the experimental surface temperature. In the AIMDEF simulations, the initial coordinates and velocities are sampled from pre-equilibrated four-layer Cu slabs, in which the atom positions and velocities in the upper three layers are representative of a Cu(111) surface at the experimental T_s. The procedure used has been described in ref 21. The AIMDEF calculations used a value of the surface lattice constant that corresponds to a bulk lattice constant of 3.698 Å, based on the calculated SRP48 value of the static lattice constant of bulk copper and the experimentally determined thermal expansion of copper at 400 K[51,52] as described in ref 21. Initial positions and velocities were sampled from 1000 different snapshots from 10 equilibrated surfaces (10000 snapshots in total). The 10 surfaces, from which coordinates and velocities were sampled, are characterized by an average surface temperature of 399.5 K. The distribution of surface temperatures characterizing the 10 surfaces exhibited a standard deviation of 60 K.

2.7.3. Trajectory Calculations. In all methods used, the equations of motion were solved with the Beeman algorithm[53] as implemented in refs 33 and 54. This has the advantage that the coordinates and velocities are available to high accuracy at the same points in time. This is relevant to, for instance, the accurate calculation of the electronic friction forces, which require the coordinates and velocities to be available to high accuracy at the same point in time (because friction forces are

DOI: 10.1021/acs.jpcc.7b01096
J. Phys. Chem. C 2017, 121, 13617−13633

based on atomic velocities and positions, where the latter determine the friction coefficients).

The AIMDEF calculations were performed with a user-modified version of the ab initio total energy and molecular dynamics program VASP (version 5.4) developed at the Universität Wien.[55,56] In the DFT calculation of the forces, the ultrasoft pseudopotentials[56,57] were used in combination, with which the SRP48 functional was parametrized for H_2 + Cu(111).[21] The AIMDEF calculations on H_2 + Cu(111) used a time step of 0.25 fs. All other details of the AIMD and DFT calculations are the same as described in ref 21.

2.7.4. Other Numerical Details. In the GLO calculations, the surface phonon frequencies ω_i were taken equal to 14 meV for $i = x, y, z$, where 14 meV is equal to the surface Debye frequency of Cu(111),[58] as used before in refs 22 and 58. The same value of the (surface) Debye frequency was used in eq 8 to calculate the phonon friction coefficient η_{ph} (see section 2.3).

In the GLO+F calculations, the electronic density of the bare Cu(111) surface, which is needed to compute the friction coefficients, was calculated from a three-dimensional cubic spline interpolation using a previously prepared spline fit. In the AIMDEF calculations, the electronic density was calculated instead from the self-consistent density of the entire H_2 + Cu(111) system with displaced Cu atoms, with subtraction of the densities due to the H atoms using a Hirshfeld partioning scheme,[26,27,59] which was also used in ref 60. Electronic friction coefficients for H atoms were obtained in the usual way[37,38,61] by computing the phase shifts of Kohn−Sham orbitals at the Fermi momentum for a proton embedded in a free electron gas for different values of the electronic embedding densities. The friction coefficients were parametrized through

$$\eta_{el,i} = (8.25 \times 10^{-8}) r_s^{10.082} \exp(-1.189 r_s) + 0.651\, r_s^{0.376} \exp(-0.605 r_s) + (6.22 \times 10^{-4})\, r_s^{-14.017} \exp(2.477 r_s) \quad (13)$$

using a fit expression used earlier in ref 25, and employing atomic units. eq 13 accurately describes the friction coefficient for values of the free electron radius r_s ranging from 1 to 10 bohrs, which covers the range relevant to our calculations.

3. RESULTS AND DISCUSSION

3.1. Comparison of the GLO+F and AIMDEF Methods. Vibrational excitation probabilities $P(v = 0, j = 5 \rightarrow v = 1, j = 3)$ computed with the AIMDEF method and the GLO+F method for H_2 + Cu(111) and T_s = 400 K are compared in Figure 2 and Table 2. As is the case for all other AIMDEF results shown in this paper, the results are obtained for the conditions relevant to the experiments (i.e., the quoted value of T_s and $\theta_i = 15°$ with incidence along the $[1\bar{2}1]$ azimuth[7]), and $j = 5$ was selected because the initial $(v = 0, j = 5)$ state makes the largest contribution (see Figure 3 of ref 16) to the gain peak (see Figure 1) in the TOF spectrum. The GLO+F results reproduce the AIMDEF results rather closely for the incidence energies $E_i \leq 0.83$ eV most important to describing the gain peak. For flight times corresponding to $E_i > 0.83$ eV, the "blue" (high-energy, short-time) tail of the gain peak drops off rather quickly, due to the exponentially decreasing amount of molecules present in the incident beam with these high E_i values.[7] The somewhat diminished accuracy with which the GLO+F method describes vibrational excitation at these E_i values should therefore be less relevant, and we conclude that

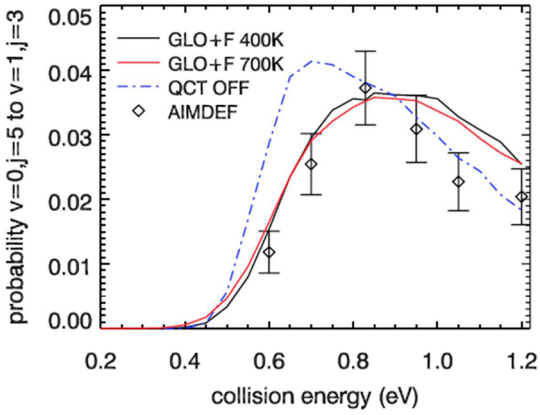

Figure 2. $P(v = 0, j = 5 \rightarrow v = 1, j = 3)$ as computed with the QCT method, with the GLO+F method for 400 and 700 K, and with AIMDEF for 400 K. The error bars on the AIMDEF results denote 68% confidence intervals.

Table 2. AIMDEF and GLO+F Results for Off-Normal Incidence at E_i = 0.829 eV and T_s = 400 K

	AIMDEF	GLO+F
$P(v = 0, j = 5 \rightarrow v = 1, j = 3)$	0.037 ± 0.006	0.0354
E_t of $(v' = 1, j' = 3)$ H_2 (eV)	0.417 ± 0.019	0.429
E_{tp} of $(v' = 1, j' = 3)$ H_2 (eV)	0.399 ± 0.019	0.407

the GLO+F method may justifiably be used to explore the effect of a range of factors on the computed TOF spectrum. The diminished accuracy of the GLO+F method for higher E_i might be due to this method being less capable of describing the more elaborate surface deformation that could occur at such energies. AIMDEF is intrinsically capable of describing surface deformation involving more than one atom, whereas the GLO +F method is not.

The energy lost by scattered H_2 is relevant to the interpretation of the experiments on vibrational excitation to $(v = 1, j = 3)$,[7] because it determines the velocity with which H_2 travels through the detection zone,[16] where H_2 is laser-excited with REMPI. The final translational energy E_t of $(v' = 1, j' = 3)$ H_2 obtained upon scattering of $(v = 0, j = 5)$ H_2 at E_i = 0.829 eV is shown in Table 2, comparing AIMDEF and GLO+F results for T_s = 400 K. As can be seen, the AIMDEF and GLO +F results for E_t are in excellent agreement with one another for this E_i. The same is true for the final translational energy in the scattering plane, E_{tp} (see also Table 2). In Table 3, we compare not only the calculated values of E_{tp}, but also the standard deviations associated with the distributions of these energies for two different values of E_i. The GLO+F method correctly predicts not only the average E_{tp} (Tables 2 and 3), but also the standard deviations of the distributions of these

Table 3. AIMDEF and GLO+F Results Compared for Off-Normal Incidence and Scattering from $(v = 0, j = 5)$ to $(v = 1, j = 3)$ at the Values of E_i Indicated and T_s = 400 K[a]

	AIMDEF	GLO+F
E_{tp} (eV) at E_i = 0.6 eV	0.33 (0.07)	0.33 (0.07)
E_{tp} (eV) at E_i = 1.05 eV	0.48 (0.17)	0.49 (0.14)

[a]The first number presented is the average E_{tp} value, and the second number (in parentheses) is the standard deviation of the distribution of E_{tp} (see the text for its definition).

DOI: 10.1021/acs.jpcc.7b01096
J. Phys. Chem. C 2017, 121, 13617−13633

energies (Table 3), suggesting that the GLO+F method is capable of correctly predicting the distributions of the final translational energies in scattering and therefore also the loss of energy to the surface phonons and to ehp's.

Dissociative chemisorption probabilities computed with the AIMDEF and GLO+F methods for ($v = 0, j = 5$) H_2 + Cu(111) and T_s = 400 K are compared in Figure 3. As can be seen,

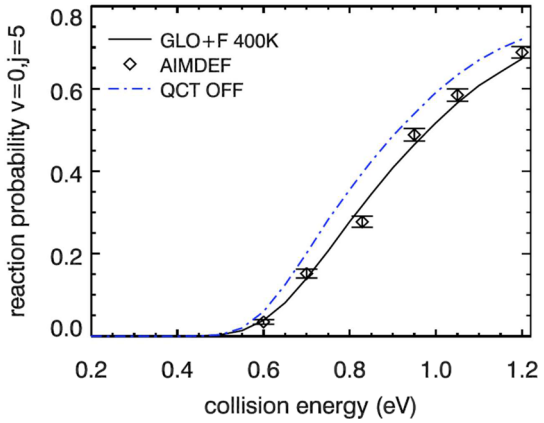

Figure 3. Reaction probability as computed for off-normal incidence with the QCT method, the GLO+F method for 400 K, and AIMDEF for 400 K for ($v = 0, j = 5$) H_2 + Cu(111). The error bars on the AIMDEF results denote 68% confidence intervals.

compared to AIMDEF, the computationally much less expensive GLO+F method yields quite accurate results for the reaction. Including the effects of phonon motion as well as ehp excitation leads to a much larger broadening of the H_2 reaction probability curve (relative to the QCT static surface result) than obtained when QCT static surface results are compared to AIMD results for D_2 + Cu(111),[20] where the effects of phonons should actually be larger for the heavier D_2. This is important, as the latter broadening was observed to be much smaller[20] than measured experimentally[62−64] for D_2 + Cu(111). The above results suggest that ehp excitation should be taken into account for a correct description of the broadening effect of increasing T_s on the reaction probability curve for H_2/D_2 + Cu(111) and that this effect can be obtained just as well with GLO+F as with AIMDEF.

Finally, probabilities $P(v = 0, j = 5 \rightarrow v', j')$ are shown for several v' and j' states for E_i = 0.829 eV in Figure 4. As can be seen, the GLO+F results are in quite good agreement with the AIMDEF results for this E_i. Together, Figures 3 and 4 help to understand why the GLO+F method is quite accurate for computing state-to-state probabilities for scattering to the (v = 1, j = 3) state: the GLO+F method is also quite capable of describing the competition of reaction and of scattering to other rovibrational states with scattering to ($v = 1, j = 3$).

3.2. TOF Spectra Simulated with Scattering Calculations Performed for Normal Incidence. To investigate the reliability of the quasi-classical approximation for computing TOF spectra for comparison with the experiments on vibrational excitation,[7] the TOF spectrum computed with the QCT method is compared to that computed with QD in Figure 5. To account for the fact that the experiments were done for off-normal incidence, in the simulation of the TOF spectra, the assumption was made that the vibrational excitation probabilities only depend on the total translational energy, and not on the incidence angle (total energy scaling, or TES). This

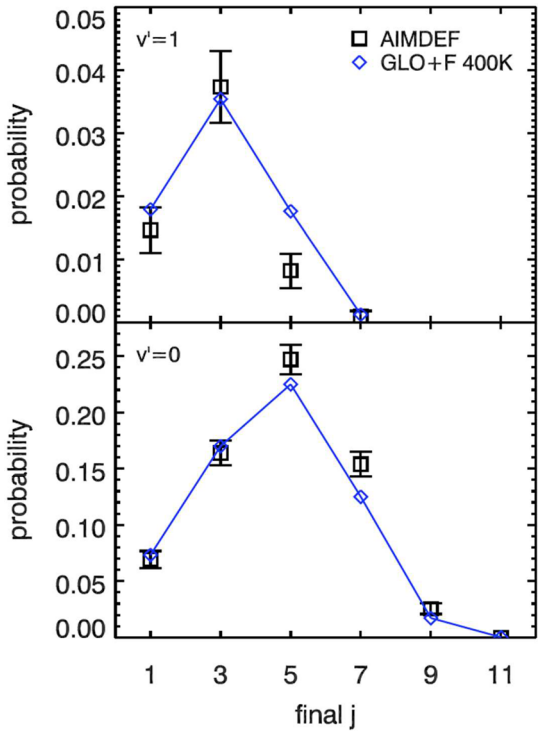

Figure 4. $P(v = 0, j = 5 \rightarrow v', j')$ as a function of j' for E_i = 0.829 eV as computed with the GLO+F and AIMDEF methods for 400 K and for v' = 1 (upper panel) and v' = 0 (lower panel). The error bars on the AIMDEF results denote 68% confidence intervals.

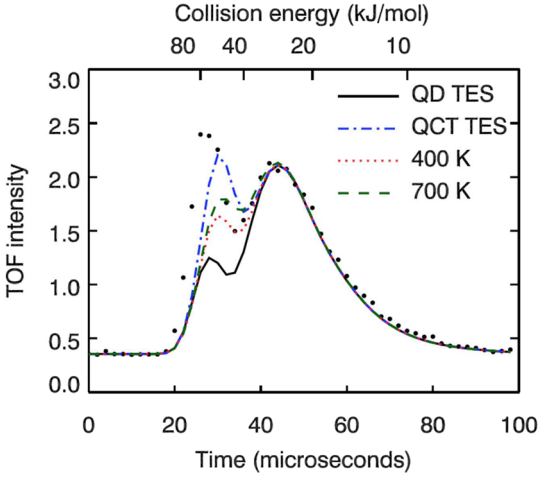

Figure 5. TOF spectra simulated from calculations performed for normal incidence with the TDWP method (QD), the QCT method, and the GLO+F method for T_s = 400 and 700 K, assuming total energy scaling (TES) of vibrational excitation. No energy loss to the surface was taken into account. The black dots denote the experimental TOF spectrum at T_s = 400 K.[7]

approximation allows the dynamics calculations to be performed for normal incidence only, which was favorable for the earlier QD, time-dependent wave packet (TDWP) calculations.[16] While the TDWP method allows results to be obtained for a range of incidence energies in just one wave packet propagation,[65] this only applies to a calculation with a fixed initial parallel momentum,[66] making the simulation of TOF spectra based on QD calculations performed for off-normal incidence expensive.

DOI: 10.1021/acs.jpcc.7b01096
J. Phys. Chem. C 2017, 121, 13617−13633

We first note that the QCT method quite well reproduces the long-time loss peak in the TOF spectrum calculated with QD. This suggests that the QCT method correctly accounts for the loss of intensity in the TOF spectrum of (v = 1, j = 3) H_2 due to reaction and vibrational de-excitation from v = 1 to v = 0 and that it correctly describes rotationally inelastic scattering within v = 1. However, the QCT calculations do not reproduce the QD short-time gain peak, which reflects vibrational excitation. Figure 6 shows that this is due to the QCT method

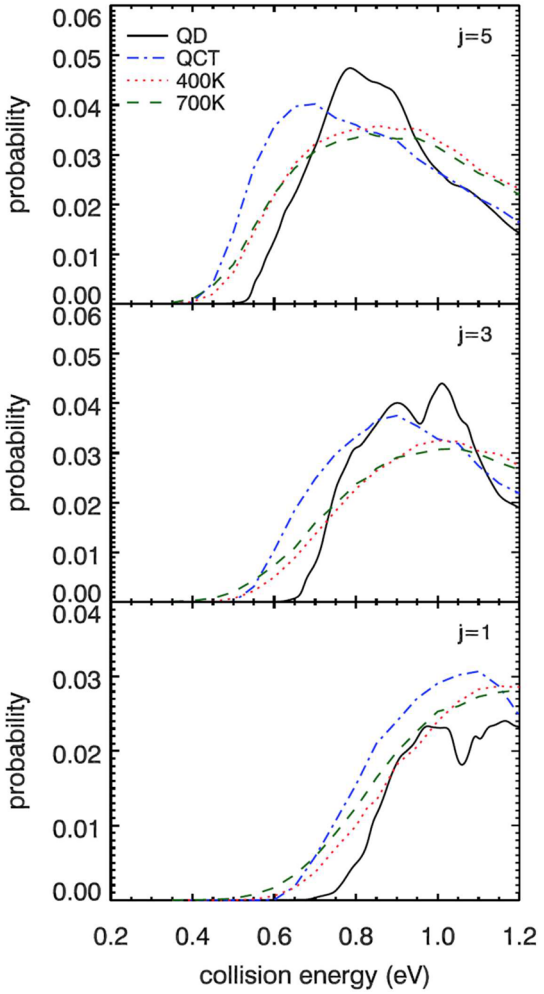

Figure 6. $P(v = 0, j \rightarrow v = 1, j = 3)$ as computed for normal incidence with the TDWP method (QD), the QCT method, and the GLO+F method for T_s = 400 and 700 K and for j = 1 (lower panel), 3 (middle panel), and 5 (upper panel).

overestimating $P(v = 0, j \rightarrow v = 1, j = 3)$ at low E_i for j = 1, 3, and 5. As a result, the height of the gain peak increases considerably at long flight times (low E_i). While this brings the peak height into better agreement with experiment, the peak position is shifted to too long flight times (to too low E_i).

The level of agreement achieved between QCT and QD for the $P(v = 0, j \rightarrow v = 1, j = 3)$ is disappointing in view of the expectation voiced in ref 16 that the vibrational excitation probabilities should be reasonably well described with QCT for $E_i \geq 0.8$ eV. This expectation was based on calculations performed on H_2 + Cu(110) using a PES calculated with the PW91 functional.[23] Being calculated with the PW91 functional, this PES most likely[19] contains a too low barrier for dissociation. Already near E_i = 0.8 eV, the vibrational excitation probability $P(v = 0, j = 0 \rightarrow v = 1, j = 0)$ computed in ref 23 took on much higher values (close to 0.1) than observed here for vibrational excitation to (v = 1, j = 3) (see Figure 6), making it easier to reproduce QD results with the QCT method (the QCT method generally performing better for larger probabilities). The rather poor performance of the QCT method for calculating probabilities $P(v = 0, j \rightarrow v = 1, j = 3)$ for low E_i for our system and PES represents a setback, as it impairs our capability of accurately simulating the "red" (i.e., low-E_i, long-time) side of the gain peak in the TOF spectrum. However, we may still hope that the effects of the incidence angle, and of allowing energy transfer to surface phonons and ehp's, are reasonably well described with quasi-classical mechanics, taking the QCT result for normal incidence as the reference. In doing so, we keep in mind that the QCT calculations (and most likely also the GLO+F calculations) are likely to overestimate the gain peak at its low-energy side. In the future, it should be worthwhile to investigate whether better results can be obtained with more sophisticated binning methods for assigning the final vibrational state[67] than used here in the QCT calculations.

To investigate the role of T_s and of allowing energy exchange with the surface, the TOF spectra computed with the GLO+F method are compared with the spectrum computed with the QCT method in Figure 5 for T_s = 400 and 700 K. It is gratifying to see that the GLO+F results qualitatively reproduce the experimental finding[7] that the height of the gain peak increases with T_s increasing from 400 to 700 K (see also Figure 1). This finding can be explained by the $P(v = 0, j \rightarrow v = 1, j = 3)$ calculated with GLO+F being higher at low E_i for T_s = 700 K than for T_s = 400 K for j = 1, 3, and 5, especially for j = 1 and 3 (see Figure 6).

However, it is disturbing to see that the gain peak obtained with the GLO+F method for T_s = 400 K is much lower than that computed with the QCT method, which uses the static surface approximation. In ref 16, the effect of T_s was estimated by assuming that the static surface results obtained with TDWP calculations should approximately equal the results for a 0 K surface in which the surface atoms are allowed to move. To estimate how results for a 400 K surface should differ from results obtained with the static surface approximation, the assumption was made that the T_s dependence of the vibrational excitation probabilities, as inferred from the differences in the observed peak height for 400 and 700 K, could be extrapolated from 400 to 0 K. More specifically, the observation of a 20% increase in the gain peak on going from T_s = 400 K to T_s = 700 K was interpreted as evidence that the gain peak should rise by 27% on going from the static surface (0 K) result to the 400 K result.[16] The results of Figure 5 show the opposite trend: the peak height is decreased on going from the static surface QCT result to the 400 K GLO+F result. This result suggests a rather limited potential of surface motion to account for the observed discrepancies between the experimental and previous theoretical results for vibrational excitation of H_2 scattering from Cu(111). A *caveat* here is that the result obtained of course depends on at which E_i the QCT and GLO+F vibrational excitation probabilities cross. We have assumed that this crossing point is reliably obtained by taking the QCT result as the standard to measure the GLO+F results against for taking into account the effects of T_s and of allowing surface motion. Since we know that the QCT method does not accurately

DOI: 10.1021/acs.jpcc.7b01096
J. Phys. Chem. C 2017, 121, 13617−13633

reproduce the QD results at low E_i, these assumptions may not be entirely correct and require testing in future work.

Figure 7 shows the effect of taking into account that the (v' = 1, j' = 3) H_2 molecules lose energy to the surface phonons and

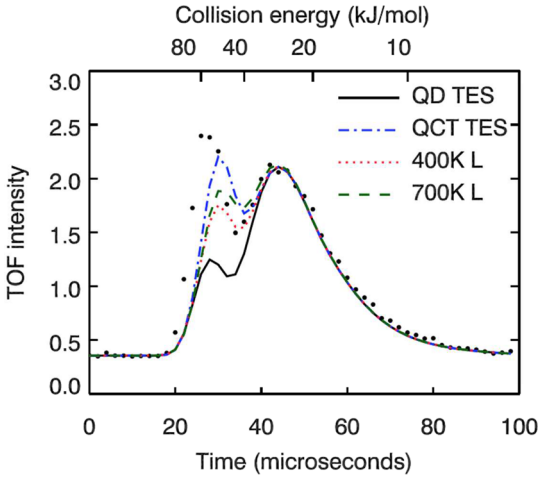

Figure 7. TOF spectra simulated from calculations performed for normal incidence with the TDWP method (QD), the QCT method, and the GLO+F method for T_s = 400 and 700 K. Energy loss to the surface was taken into account in the GLO+F results. The black dots denote the experimental TOF spectrum at T_s = 400 K.[7]

through ehp excitation, which ensures that the molecules fly less quickly through the detecting laser beam, making detection more likely, in the GLO+F calculations. For T_s = 400 K and E_i = 0.829 eV, depending on j, energy losses were in the range of 18−26% of the available energy ($E_i - E_{th}$), where E_{th} is the threshold E_i for vibrational excitation to the (v = 1, j = 3) state of H_2 in the BOSS model (see also eq 2). This ensures that for the GLO+F calculations the gain peaks in Figure 7 are somewhat higher than in Figure 5. Whereas the energy loss percentages calculated with GLO+F are somewhat smaller than assumed in a previous analysis (i.e., 30%),[16] the results of Figure 7 show that allowing energy loss to "surface modes" such as phonons and ehp's does lead to a modest increase in the height of the gain peak attributed to vibrational excitation. This partly accounts for the differences previously observed between QD and experimental results for vibrational excitation of H_2 scattering from Cu(111) (see also below for the results for off-normal incidence).

3.3. TOF Spectra Simulated with Scattering Calculations Performed for Off-Normal Incidence. The experiments were performed for θ_i = 15° with incidence along the [1$\bar{2}$1] azimuth.[7] However, previous QD calculations simulated TOF spectra from vibrational excitation probabilities computed for normal incidence. This required assumptions about whether at off-normal incidence the vibrational excitation probabilities should scale with the normal or total incidence energy or whether an intermediate scaling would be obeyed.[16] To investigate whether the assumptions made were correct, here we also performed QCT calculations for off-normal incidence for the experimental conditions. Figure 8 shows that the gain peak obtained in this way is much closer in height to the result obtained from QCT normal incidence results assuming normal energy scaling (NES) than that obtained assuming total energy scaling (TES).

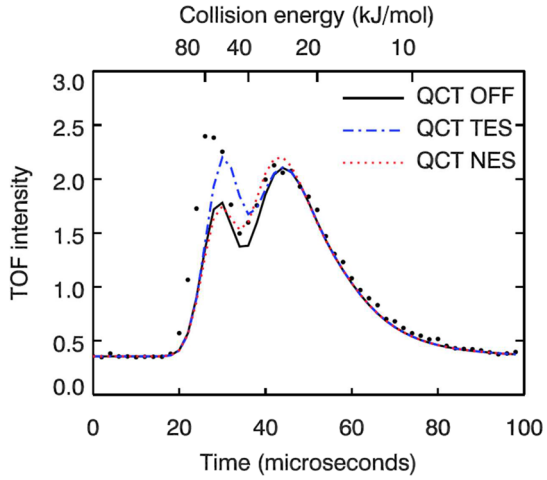

Figure 8. TOF spectra calculated with the QCT method for off-normal incidence (15° off-normal, QCT OFF) and with the QCT method from normal incidence results assuming total energy scaling (QCT TES) or normal energy scaling (QCT NES). The black dots denote the experimental TOF spectrum at T_s = 400 K.[7]

Figure 9 shows that at low E_i the $P(v = 0, j \rightarrow v = 1, j = 3)$ values computed for off-normal incidence from normal incidence results assuming TES are larger than the $P(v = 0, j \rightarrow v = 1, j = 3)$ values computed directly for off-normal incidence (OFF) for j = 1−5. This explains why the gain peak computed from normal incidence results assuming TES is too high compared to the QCT result obtained directly for the actual incidence conditions. A previous quantum dynamical result obtained directly for the experimental off-normal incidence condition suggested that, in the range of E_i of interest, the vibrational excitation probabilities should fall midway between the probabilities computed from normal incidence results assuming TES and NES ("intermediate scaling").[16] However, the off-normal incidence result was obtained for only one value of E_i (0.83 eV) and for one value of j (j = 3). The present work suggests that the assumption about the scaling being intermediate between TES and NES does not necessarily hold and that at low E_i it might be better to assume NES than intermediate scaling as done earlier.[16] Relative to the earlier work, this should lead to increased discrepancies between theory and experiment for the gain peak; i.e., the computed gain peak, which was already too small, should be further reduced by a factor of 1.25.[16] The present work also suggests that it should be better to obtain QD results for off-normal incidence. This could be done by performing TDWP calculations for several values of the initial momentum parallel to the experimental [1$\bar{2}$1] incidence plane[7] and interpolating these results to get results for the range of E_i of interest to the experiments. With present day computational resources, this should now be feasible.

The TOF spectrum obtained from off-normal incidence results computed with the GLO+F method for T_s = 400 K is compared to the QCT static surface result and the GLO+F spectrum computed for 700 K in Figure 10. In the computation of the gain peak in the TOF spectrum based on the GLO + F results, all energy losses out of the translational motion in the incident plane were taken into account, now also including loss to translational motion out of the scattering plane. Depending on the initial value of j, energy losses ranged from 21% to 36% (see Table 4), in reasonable agreement with the value of 30%

DOI: 10.1021/acs.jpcc.7b01096
J. Phys. Chem. C 2017, 121, 13617−13633

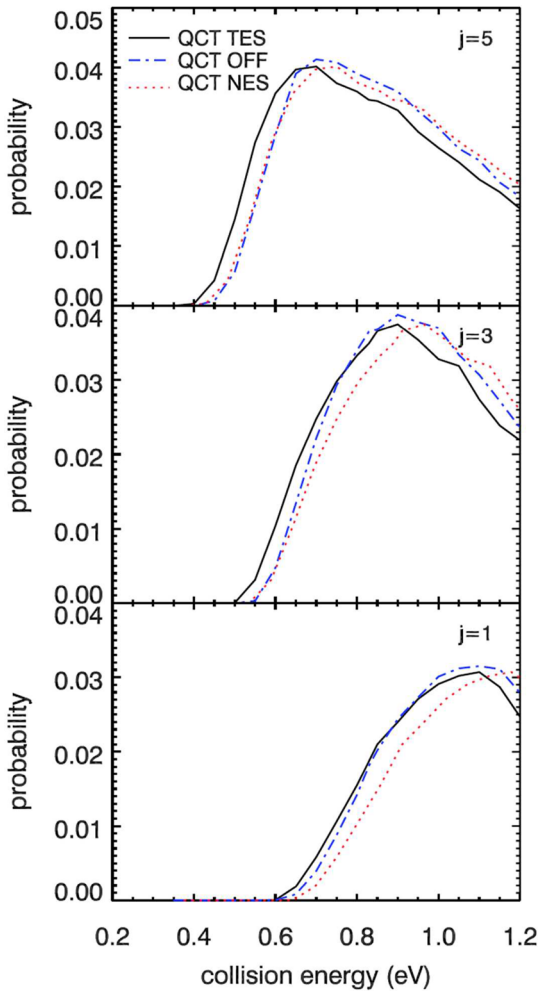

Figure 9. $P(v = 0, j \rightarrow v = 1, j = 3)$ for off-normal incidence as computed with the QCT method directly (QCT OFF) and from normal incidence QCT results assuming total energy scaling (QCT TES) or assuming normal energy scaling (QCT NES) for T_s = 400 K and for j = 1 (lower panel), 3 (middle panel), and 5 (upper panel).

assumed in earlier work.[16] Energy losses to translation outside the scattering plane contribute 5−14% to these percentages. Note that we have verified that the fractional energy loss to phonons, ehp's, and motion out of the scattering plane is, to a reasonable extent, independent of E_i.

As also found for normal incidence (Figure 7), the GLO+F gain peak for T_s = 400 K is lower than the QCT gain peak, even though energy losses are taken into account in the GLO+F calculations but not in the QCT calculation of the TOF peak. The reason is the same as for normal incidence: the GLO+F vibrational excitation probabilities are smaller than the QCT probabilities for the initial j values that are important to the calculation of the gain peak and the low E_i values relevant to the gain peak (see Figure 11).

It is of interest to see whether modeling ehp excitation (using the GLO+F rather than the GLO method) leads to an increase in the gain peak in the TOF spectrum, which one would then normally attribute to increased vibrational excitation. As can be seen from Figure 12, this is not the case: for the value of T_s at which most experiments were done (400 K), modeling ehp excitation leads to a *lower* gain peak. The reason is that for the important initial j states ($j \leq 5$) and the E_i values most relevant to the calculation of the gain peak (≤0.9 eV) the computed

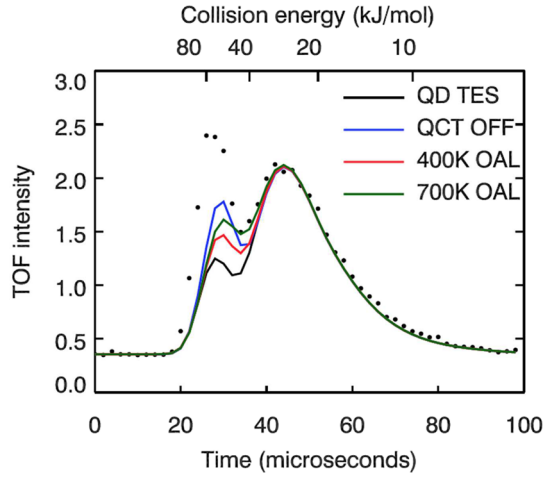

Figure 10. TOF spectra calculated from results for scattering at off-normal incidence with the TDWP method (QD TES, from normal incidence results assuming TES), the QCT method (QCT OFF), and the GLO+F method for T_s = 400 and 700 K (400 K OAL and 700 K OAL). All energy losses (to the surface and to motion out of the scattering plane) were taken into account in the GLO+F results. The black dots denote the experimental TOF spectrum at T_s = 400 K.[7]

vibrational excitation probabilities decrease if friction is introduced (see Figure 13). This effect is more important than the extra translational energy loss to friction, which leads to increased detection because the vibrationally excited H_2 flies more slowly through the detection zone (see Table 4, noting that the translational energy loss is larger in GLO+F than in GLO for T_s = 400 K). Apparently, the effect that the molecule has already lost some energy to ehp excitation when it hits the surface leads to decreased vibrational excitation at the lower E_i, and the ensuing effect on the gain peak is larger than the increased detection following from the energy loss to ehp excitation.

One might also ask what the effect on the gain peak (and on vibrational excitation) is of raising T_s and whether this depends on whether ehp excitation is modeled. The answer to this question is rather surprising. Even though the effect of ehp excitation is to decrease the gain peak and vibrational excitation at lower E_i for T_s kept fixed, raising T_s only leads to a considerable increase in the height of the gain peak and to increased vibrational excitation if ehp excitation is included! This can be seen by comparison of Figure 14 (showing TOF spectra computed with the GLO method) with Figure 10 (showing TOF spectra computed with the GLO+F method). Just heating the phonons from 400 to 700 K hardly raises the gain peak (Figure 14), whereas heating the phonons *and* the electrons does (Figure 10). This GLO+F effect of raising T_s does not come from more efficient detection due to greater loss of translational energy; in fact, the percentages of energy loss to the surface are smaller for 700 K (Table 4). Instead, the effect arises from the $P(v = 0, j \rightarrow v = 1, j = 3)$ calculated with the GLO+F method being larger for 700 K than for 400 K for low j and the relevant low E_i, especially for j = 1 and 3 (see Figure 11). In contrast, the $P(v = 0, j \rightarrow v = 1, j = 3)$ values calculated for low initial j with the GLO method are more or less the same for 400 and 700 K (see also Figure 11). We attribute the effect of raising T_s on the vibrational excitation probabilities computed with GLO+F to the concomitant greater random force exerted by the electrons on the H nuclei in the region of configuration space where the electronic friction coefficients are

DOI: 10.1021/acs.jpcc.7b01096
J. Phys. Chem. C 2017, 121, 13617−13633

Table 4. Energy Losses for Off-Normal Incidence GLO+F Calculations for T_s = 400 and 700 K and E_i = 0.829 eV[a]

j	$E_i - E_{th}$	E_{QCT}	$E_{GLO+F,\ 400\ K}$	energy loss (%)	$E_{GLO+F,700\ K}$	energy loss (%)
1	0.2447	0.402	0.351 (0.364)	21 (16)	0.371	13
3	0.3175	0.445	0.368 (0.395)	24 (16)	0.388	18
5	0.4456	0.518	0.407 (0.446)	25 (16)	0.421	22
7	0.6246	0.669	0.480 (0.545)	30 (20)	0.487	29
9	0.8461	0.875	0.588 (0.689)	34 (22)	0.595	33
11	1.0471	1.115	0.743 (0.857)	36 (25)	0.740	36

[a]E_{QCT} is the total final translational energy obtained with QCT calculations. $E_{GLO+F,\ 400\ K}$ is the translational energy for motion in the scattering plane as obtained with GLO+F for T_s = 400 K, and $E_{GLO+F,700\ K}$ is the same obtained for T_s = 700 K. The energy loss (%) is obtained by taking the difference of E_{GLO+F} and E_{QCT} and dividing by ($E_i - E_{th}$). All energies are in electronvolts. Values in parentheses are for GLO calculations for 400 K.

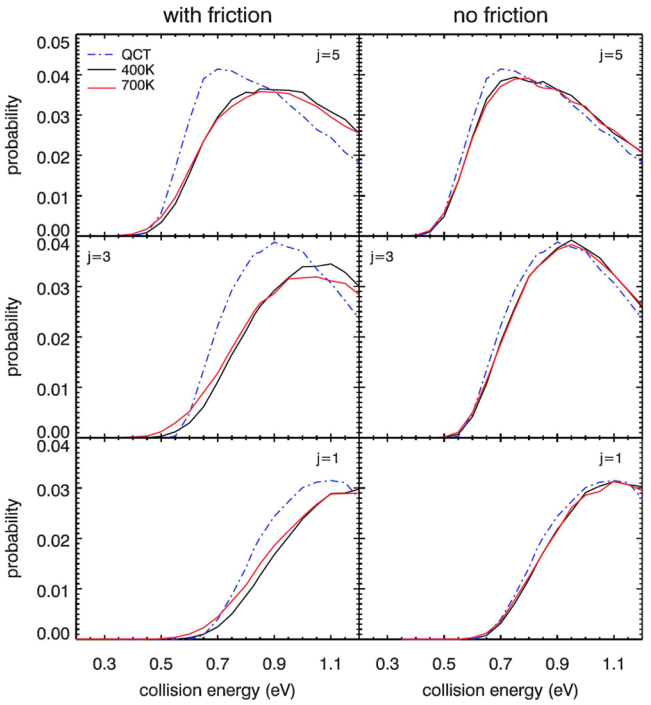

Figure 11. $P(v = 0, j \rightarrow v = 1, j = 3)$ for off-normal incidence as computed directly with the QCT method (QCT) and with the GLO +F method (left) or the GLO method (right) for T_s = 400 and 700 K and for j = 1 (lower panels), 3 (middle panels), and 5 (upper panels).

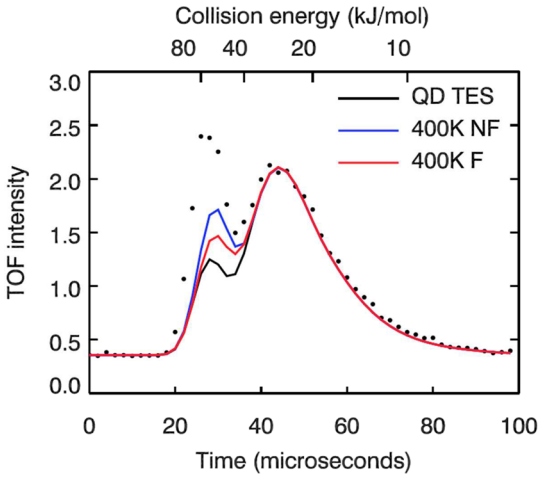

Figure 12. TOF spectra calculated from the results for scattering at off-normal incidence with the TDWP method (QD TES, from normal incidence results assuming TES), the GLO+F method (400 K F), and the GLO method (400 K NF) for T_s = 400 K. Energy loss to the surface and to motion out of the scattering plane was taken into account in the GLO and GLO+F results. The black dots denote the experimental TOF spectrum at T_s = 400 K.[7]

large (see eq 11). The rise in the gain peak seen in the GLO+F calculations (Figure 10) is in qualitative agreement with experimental observations[7] (see Figure 1), and our analysis suggests that the experimentally observed increase of the gain peak with T_s can be attributed to an electronically nonadiabatic mechanism. However, it would be good to check in future research whether a phononic contribution to the rise of the gain peak with T_s would result from AIMD calculations, which treat the phonons in a more sophisticated way. Such calculations would probably need to employ a much larger number of AIMD trajectories than used here, to make the statistical error bars small enough to enable the detection of potential, reasonably sized phononic contributions to the rise of the gain peak with T_s.

3.4. Effects of Uncertainties in Computed Vibrational Excitation Probabilities and Time Origin in Experiment on the TOF Spectrum. In section 3.2 we saw that uncertainties in computed vibrational excitation probabilities (in this case, due to the use of the classical approximation in the QCT calculations) can lead to large changes in the computed TOF spectrum. For this reason, we decided to explore two factors that might affect the TOF spectrum.

The first effect we explored concerns the calculations. It is conceivable that, due to errors in the PES (for instance, in the reaction barriers), the vibrational excitation probabilities should be shifted to lower incident translational energies. To explore this, we took the original quantum dynamical vibrational excitation probabilities (see, e.g., Figure 6) and shifted them to lower energies by 1 kcal/mol (~43 meV). Figure 15 shows how this alters the gain peak in the TOF spectrum relative to the original QD results, in both cases assuming that at off-normal incidence the vibrational excitation probabilities obey TES. The shifts along the energy axis lead to a substantial increase in the height of the gain peak (Figure 15), which is due to the strong dependence of the TOF signal on the incident velocity distribution (see eq 1). If additionally an energy loss of 30% is assumed (as done originally in ref 16 and justified to a large extent by our GLO+F results; see section 3.3 and Table 4), the peak is further increased (Figure 15). If additionally the gain peak is multiplied by a factor of only 1.5, already quite good agreement is obtained with experiment for the height of the gain peak (see also Figure 15). To be fair, it should be noted that our present calculations suggest that it should be better to assume NES than TES and that this should change[16] the multiplication factor required for good agreement of the peak height with experiment to a factor of 2.2.

DOI: 10.1021/acs.jpcc.7b01096
J. Phys. Chem. C 2017, 121, 13617−13633

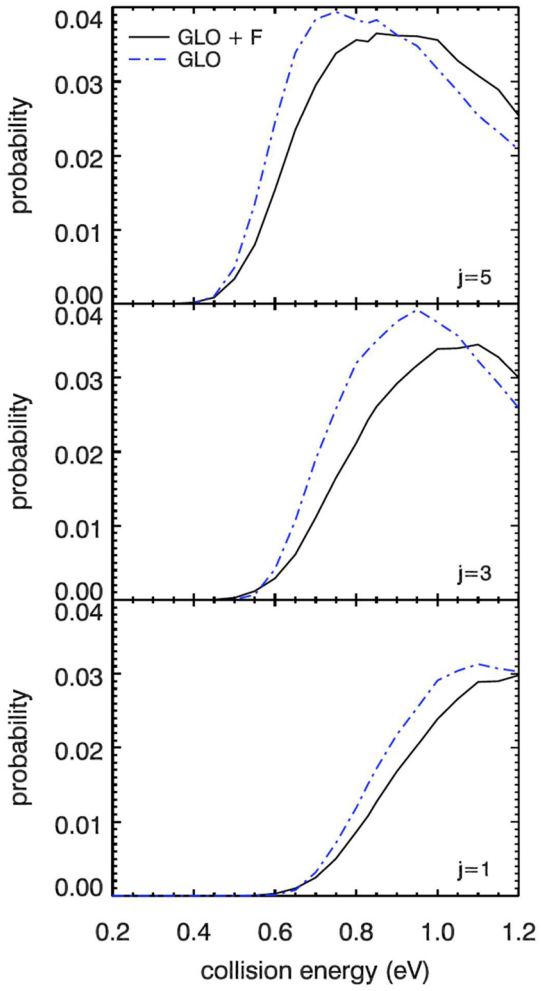

Figure 13. $P(v = 0, j \rightarrow v = 1, j = 3)$ for off-normal incidence as computed directly with the GLO+F and GLO methods for $T_s = 400$ K and for $j = 1$ (lower panel), 3 (middle panel), and 5 (upper panel).

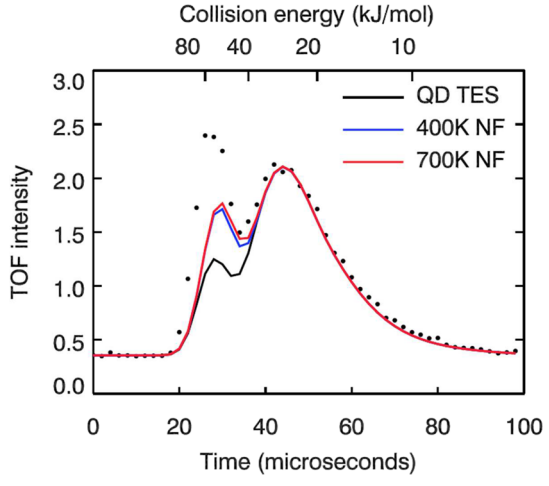

Figure 14. TOF spectra calculated from the results for scattering at off-normal incidence with the TDWP method (QD TES, from normal incidence results assuming TES) and with the GLO method for T_s = 400 and 700 K (400 K NF and 700 K NF). Energy loss to the surface and to motion out of the scattering plane was taken into account in the GLO results. The black dots denote the experimental TOF spectrum at $T_s = 400$ K.[7]

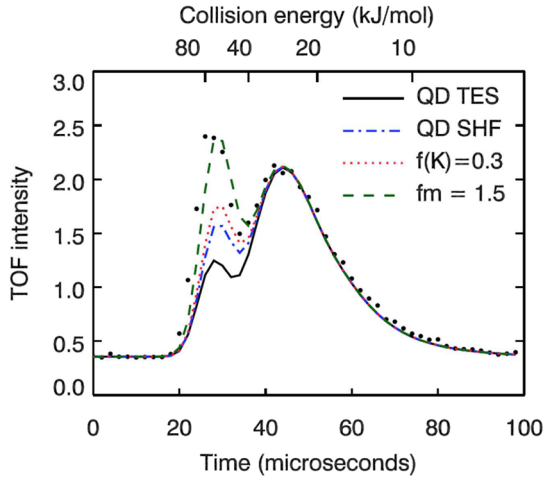

Figure 15. TOF spectra calculated with the TDWP method on the basis of the original QD vibrational excitation probabilities (QD TES), on the basis of the QD vibrational excitation probabilities shifted along the incident energy axis by −1 kcal/mol (QD SHF), additionally assuming 30% energy loss ($f(K) = 0.3$), and additionally multiplying the shifted probabilities by a factor of 1.5 (fm = 1.5). The black dots denote the experimental TOF spectrum at $T_s = 400$ K.[7]

The gain peak obtained by shifting the QD vibrational excitation probabilities by −1 kcal/mol is not yet in the right position; i.e., it occurs at a too low energy (too long time of flight), as may be seen from Figure 15. However, the experiments also contain an uncertainty of about 1 μs, which is due to a lack of perfect timing in comparing reference and scattered TOF distributions.[7] To see the possible effect of such a shift, we additionally shifted the time origin by −1 μs. The effect of this additional shift is shown in Figure 16. As may be seen, the position of the peak is now also in the approximately correct place. In other words, shifting the vibrational excitation probabilities by −1 kcal/mol in incident translational energy and shifting the time origin by a value within the experimental

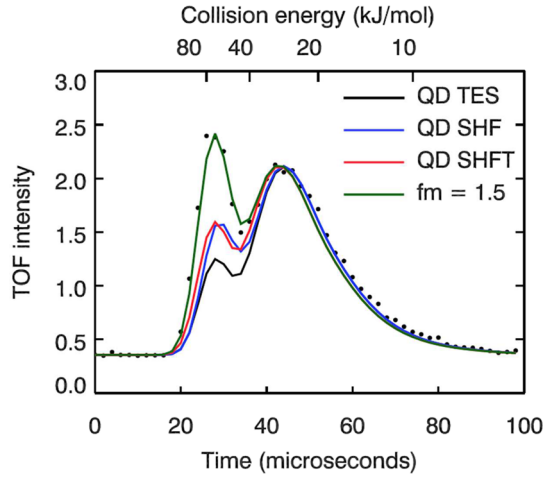

Figure 16. TOF spectra based on the original QD vibrational excitation probabilities (QD TES), on QD vibrational excitation probabilities shifted along the incident energy axis by −1 kcal/mol (QD SHF), additionally applying a shift of the time origin by −1 μs (QD SHFT), and additionally assuming 30% energy loss and multiplying the shifted probabilities by a factor of 1.5 (fm = 1.5). The black dots denote the experimental TOF spectrum at $T_s = 400$ K.[7]

DOI: 10.1021/acs.jpcc.7b01096
J. Phys. Chem. C 2017, 121, 13617−13633

error (i.e., by 1 μs) leads to a TOF spectrum with the gain peak occurring at almost the correct flight time (corresponding E_i). However, the peak still needs to be multiplied by a factor of 2.2 (1.5), assuming vibrational excitation at off-normal incidence obeys normal (total) energy scaling. Nevertheless, these TOF spectrum simulations show that the position of the gain peak in the TOF spectrum is quite sensitive to both the dependence of the vibrational excitation probabilities on incidence energy and the origin of time in the measurements. The comparison of theory to experiment would clearly benefit from both a higher time resolution in the experiments and, possibly, improved accuracy of the description of the dependence of the computed vibrational excitation probabilities on the incident translational energy.

3.5. Discussion: Remaining Issues and Future Improvements. The comparison between GLO+F and AIMDEF results (Figure 2) suggests that, for modeling the TOF spectrum exhibiting vibrational excitation in the gain peak, it should be enough to use the GLO+F method and model the surface through a single oscillating atom connected to a ghost atom. In turn, this suggests that it might be possible to model the effect of (allowing) surface motion on vibrationally inelastic scattering of H_2 from Cu(111) with QD calculations in which the motion of only one surface atom connected to a bath of oscillators and ehp's is considered. This can perhaps be done in the spirit of the GLO method, for instance using a density matrix formalism[68−70] or using stochastic wave function approaches.[71−74] Before such QD calculations are carried out, it might be useful to test whether it is necessary to retain all three degrees of freedom of the surface atom or whether it might be enough just to model its motion perpendicular to the surface. Finally, the GLO+F method clearly suffices for modeling the effect of surface phonons and ehp excitation on dissociative chemisorption (Figure 3) and to calculate energy loss to the surface (Tables 2 and 3).

The present comparison between QCT and TDWP results clearly shows that QCT with box quantization of the final vibrational state, as employed here, is not of sufficient accuracy to reliably compute the gain peak representing the effect of vibrational excitation in the TOF spectrum (Figure 5). Future work should test whether better results can be obtained if more sophisticated methods, such as Gaussian binning techniques,[67] are used to assign final vibrational states to the outcome of quasi-classical trajectories. Alternatively, it might be possible to analyze the final vibrational state of the scattered molecule using a so-called adiabatic switching procedure.[75] This obviously represents an important issue, as the present work suggests that the vibrational excitation probabilities computed with methods using the quasi-classical approximation (including QCT, GLO+F, and AIMDEF) are much too high at the incidence energies relevant to the simulation of the gain peak (Figure 6). To enable a quantitatively accurate simulation of the TOF spectrum, this problem should be solved, or one should revert to the use of QD and solve the problem of how to model the effect of energy transfer involving surface phonons and ehp's with a quantum dynamical approach.

Our present QCT results for off-normal incidence strongly suggest that, within a QD approach, it should not be an accurate approximation to assume that vibrational excitation obeys NES or TES or a scaling midway between these two limits characterized by a single mixing coefficient for all times of flight (Figures 8 and 9). Rather, the calculations suggest that, in a QD approach, the calculations should be performed for off-normal incidence. This will make the QD simulation of the TOF spectrum much more expensive, as TDWP calculations will have to be performed for several values of the initial translational momentum in the plane of incidence. However, with present-day computational resources, this should now be possible, at least within the BOSS model.

Our TOF simulations based on QD vibrational excitation probabilities also show that the simulated TOF spectrum is quite sensitive to the origin of time in the experiments (Figure 16) and to the exact dependence of the vibrational excitation probabilities on E_i (Figures 15 and 16). Concerning the latter, it should be possible to remove some remaining uncertainties regarding the PES by reparametrizing an SRP functional for H_2 + Cu(111), using a correlation functional approximately describing the attractive van der Waals interaction with the surface,[76−79] as done successfully for CH_4 + Ni(111).[80] There are indications that such a functional should exhibit a somewhat higher, and later, barrier to reaction.[81] Both the higher barrier and the somewhat increased velocity toward the surface resulting from the slight acceleration in the van der Waals well (with an experimental depth of about 30 meV[82]) could lead to increased vibrational excitation and to energy shifts of the vibrational excitation probabilities, on which the simulated TOF spectra show a strong dependence (Figure 16). The use of such a reparametrized functional might also lead to an even more accurate description of the orientational dependence of reaction of D_2 on Cu(111) than the one already obtained with the SRP48 functional.[21] Additionally, with such a functional, one could also test whether the experimentally measured effect of selective adsorption resonances on scattering of H_2 from Cu(111) in the low-incidence-energy regime (<50 meV)[83] could be accurately described. Calculations using correlation functionals that describe the van der Waals interaction in at least an approximate way suggest that this should be possible,[84,85] and an empirical potential describing scattering in the van der Waals energy regime and reproducing the resonances is available from potential inversion.[83] Furthermore, an investigation[81] of H_2 + Cu(111) that considered a few experiments on H_2 + Cu(111) also addressed with the SRP and SRP48 functionals showed that these experiments were equally well described with the optimized Perdew−Burke−Ernzerhof van der Waals density functional (optPBE-vdW-DF).[86] This latter functional was not used in the present study as it has not yet been used for quantitative comparison with the same wide range of experiments as the SRP and SRP48 functionals.

Concerning new calculations, it might also be of interest to investigate how the use of tensorial friction coefficients[87,88] might alter the results compared to the present use of the LDFA-IAA method. Note, however, that tensorial frictions should be calculated in the exact quasi-static limit, which to our knowledge has not been accomplished yet.[89]

Finally, it would certainly be advantageous if additional experiments were to become available for comparison. For instance, it would already be helpful if, in experiments similar to the one we now use for comparison, the origin of time would be much better defined than the present value (of 1 μs),[7] as the TOF spectrum is quite sensitive to this value (Figure 16). As already pointed out in ref 16 it would also be advantageous to know the nozzle temperature used in the original molecular beam experiment with high accuracy: the original work stated its value (2000 K), but not its uncertainty.[7] TOF spectra simulated on the basis of TDWP calculations suggested a strong dependence of the gain peak on the experimental nozzle

DOI: 10.1021/acs.jpcc.7b01096
J. Phys. Chem. C 2017, 121, 13617−13633

temperature (see Figure 3 of ref 16). It would also be nice to have TOF spectra available for a large range of surface temperatures. This might help to determine through dynamics calculations whether the observed dependence of vibrationally inelastic scattering on this parameter can indeed be explained with an electronically nonadiabatic mechanism, as our calculations now suggest. Finally, it would be even better to be able to compare directly to individually measured state-to-state vibrational excitation probabilities $P(v = 0, j \rightarrow v = 1, j')$. Then an eventual agreement between theory and experiment could no longer be due to error cancellation between values obtained for different j values, as might have occurred in the present and earlier[16] work for the simulated TOF spectrum.

4. CONCLUSIONS AND OUTLOOK

Previous work has shown that, with the SRP-DFT functionals now available for H_2 + Cu(111), the sticking of H_2 and D_2, the dependence of associative desorption on the final rovibrational (v, j) state, rotationally inelastic scattering, and even the orientational dependence of reaction can all be described quite accurately for this system. In contrast, vibrationally inelastic scattering of H_2 from Cu(111) has so far defied an accurate theoretical description. Previous work on vibrational excitation in this system had raised several questions regarding its dependence on the incidence angle, on the surface temperature, and on allowing energy exchange with the surface and regarding the applicability of classical mechanics. Here we have tackled these questions using the QCT, GLO, GLO+F, and AIMDEF methods, employing the SRP functionals available for H_2 + Cu(111) to eliminate uncertainties due to possible inaccuracies in the molecule−surface interaction as much as possible.

The results of the present work strongly suggest that, to model the feature in experimental TOF spectra due to vibrational excitation (the so-called gain peak; see Figure 1) with reasonable accuracy, it should not be necessary to use AIMDEF to describe surface deformation on impact. Rather, it should suffice to treat energy exchange with and dissipation to the surface within a GLO+F formalism. The GLO+F calculations also accurately describe dissociative chemisorption and the competition with scattering to other rovibrational states than probed in the experiments we have used for comparison. Importantly to the simulation of the TOF spectra exhibiting the effects of vibrational excitation, compared with AIMDEF, the GLO+F calculations accurately describe energy loss to the surface, which is relevant to the detected TOF signal. The GLO +F results for energy loss (about 30%) are in good agreement with assumptions made earlier[16] about the size of the energy loss to the surface accompanying vibrational excitation of H_2 in scattering from Cu(111).

The present comparison between QCT and QD results suggests that the QCT method accurately describes the so-called loss peak in the TOF spectra, which reflects reaction and vibrational de-excitation and rotationally inelastic scattering within the vibrationally excited state. Unfortunately, the feature in the TOF spectra most relevant to this work (the gain peak due to vibrational excitation) is not described with quantitative accuracy using quasi-classical mechanics, because the QCT method overestimates the vibrational excitation probabilities for the relevant initial rotational states and (low) E_i values. However, it is possible to derive a number of important qualitative conclusions from the GLO and GLO+F results by adopting the QCT results as a reference, keeping in mind that some of these conclusions may require further checks through QD calculations, as discussed above in several places.

The GLO+F calculations reproduce the experimental finding that raising T_s from 400 to 700 K promotes vibrational excitation. Surprisingly, the comparison with GLO results for these temperatures suggests that the effect is due to an electronically nonadiabatic mechanism, in which the randomly fluctuating forces due to the hotter electrons promote vibrational excitation at the higher T_s. Earlier work had assumed that the effect should be due to a mechanism involving surface phonons.[16] The fluctuating forces referred to are based on friction coefficients, suggesting that, through comparison with experiments on nonreactive or weakly reactive systems exhibiting strongly increasing vibrational excitation with increasing T_s,[13−15] calculations might be able to test different friction models aiming to describe the effects of ehp excitation.

Importantly, the present work shows that at moderate T_s (400 K) the effect of allowing energy transfer to the surface phonons (as evident from the GLO calculations) and to ehp's (as evident from the comparison of GLO to GLO+F calculations) is to reduce vibrational excitation. Thus, on a 0 K surface, the mobility of the surface atoms and the possibility of ehp excitation ensure that the vibrational excitation is reduced relative to that found with the Born−Oppenheimer static surface (BOSS) model. This highlights the disagreement already found earlier between theoretical work and experiments on vibrational excitation, where the earlier work assumed that allowing energy transfer from the surface phonons should lead to increased vibrational excitation for the experimental 400 K surface. However, this work assumed that vibrationally inelastic scattering from a 0 K surface should essentially be equal to that occurring over a hypothetical static surface. The present work strongly suggests that this should not be the case.

The present work also suggests that, at off-normal incidence, vibrational excitation probabilities cannot be accurately computed from normal incidence calculations assuming total or normal energy scaling of these probabilities, nor can one assume a constant (i.e., independent of E_i) mixing of TES and NES to obtain results for off-normal incidence. At the E_i most relevant to the simulation of the gain peak, the scaling of the vibrational excitation probabilities is closest to NES, and this further highlights the quantitative disagreement found earlier between theoretical work and the TOF experiments on vibrational excitation.

Simulations performed on the basis of earlier QD calculations of vibrational excitation probabilities show that the gain peak is quite sensitive to a constant energy shift of calculated excitation probabilities and to the exact chopper opening time in the experiments. Applying shifts that are reasonable (by −1 kcal/mol for the vibrational excitation probabilities and −1 μs for the chopper opening time) leads to considerably improved agreement of the theory with the experiment.

Given the comparative ease with which energy transfer to the surface can be modeled with classical mechanics, we recommend that future research be directed at more accurate schemes for assigning final vibrational states in quasi-classical calculations.[67,75] It is also worthwhile to test QD schemes for incorporating energy transfer between the molecule and the surface phonons and ehp's modeled as a bath.[68−74] Finally, additional experiments, in particular aimed at obtaining fully rotationally resolved state-to-state vibrational excitation prob-

DOI: 10.1021/acs.jpcc.7b01096
J. Phys. Chem. C 2017, 121, 13617−13633

abilities, could be quite helpful for improving the theory. The present TOF experiments on vibrational excitation reflect scattering from several initial j states within $v = 0$ as well as energy losses to the surface, making the attribution of the causes of the disagreement between theory and experiment somewhat muddled.

AUTHOR INFORMATION

Corresponding Author

*E-mail: g.j.kroes@chem.leidenuniv.nl.

ORCID

Geert-Jan Kroes: 0000-0002-4913-4689

Notes

The authors declare no competing financial interest.

ACKNOWLEDGMENTS

G.-J.K. thanks the Donostia International Physics Center for their generous financial support and his coauthors for hosting his sabbatical visit. This work was supported financially by the European Research Council through an ERC-2013 advanced grant (No. 338580). M.A. and J.I.J. acknowledge financial support by Gobierno Vasco-UPV/EHU Project IT756-13 and the Spanish Ministerio de Economía y Competitividad (Grant Nos. FIS2013-48286-C02-02-P and FIS2016-76471-P). Computational resources were provided by the DIPC computing center and through an NWO-EW (Nederland Organisatie voor Wetenschappelijk Onderzoek, gebied Exacte Wetenschappen) grant of computing time on the Dutch national supercomputer.

REFERENCES

(1) Ertl, G. Primary steps in catalytic synthesis of ammonia. *J. Vac. Sci. Technol., A* **1983**, *1*, 1247−1253.

(2) Honkala, K.; Hellman, A.; Remediakis, I. N.; Logadottir, A.; Carlsson, A.; Dahl, S.; Christensen, C. H.; Nørskov, J. K. Ammonia synthesis from first-principles calculations. *Science* **2005**, *307*, 555−558.

(3) Rettner, C. T.; Auerbach, D. J.; Michelsen, H. A. Observation of direct vibrational excitation in collisions of H_2 and D_2 with a Cu(111) surface. *Phys. Rev. Lett.* **1992**, *68*, 2547−2550.

(4) Hodgson, A.; Moryl, J.; Traversaro, P.; Zhao, H. Energy transfer and vibrational effects in the dissociation and scattering of D_2 from Cu(111). *Nature* **1992**, *356*, 501−504.

(5) Darling, G. R.; Holloway, S. Translation-to-vibrational excitation in the dissociative adsorption of D_2. *J. Chem. Phys.* **1992**, *97*, 734−736.

(6) Darling, G. R.; Holloway, S. Dissociation thresholds and the vibrational excitation process in the scattering of H_2. *Surf. Sci.* **1994**, *307*−*309*, 153−158.

(7) Rettner, C. T.; Michelsen, H. A.; Auerbach, D. J. Determination of quantum-state-specific gas-surface energy transfer and adsorption probabilities as a function of kinetic energy. *Chem. Phys.* **1993**, *175*, 157−169.

(8) Watts, E.; Sitz, G. O. State-to-state scattering in a reactive system: H_2(v = 1,j = 1) from Cu(100). *J. Chem. Phys.* **2001**, *114*, 4171−4179.

(9) Kim, J.; Sitz, G. O. The sticking of H_2(v = 1,J = 1) on Cu(100) measured using laser-induced thermal desorption. *Mol. Phys.* **2010**, *108*, 1027−1032.

(10) Huang, Y.; Wodtke, A. M.; Hou, H.; Rettner, C. T.; Auerbach, D. J. Observation of vibrational excitation and de-excitation for NO (v = 2) scattering from Au(111): Evidence for electron-hole-pair mediated energy transfer. *Phys. Rev. Lett.* **2000**, *84*, 2985−2988.

(11) Huang, Y. H.; Rettner, C. T.; Auerbach, D. J.; Wodtke, A. M. Vibrational promotion of electron transfer. *Science* **2000**, *290*, 111−114.

(12) Krüger, B. C.; Meyer, S.; Kandratsenka, A.; Wodtke, A. M.; Schäfer, T. Vibrational inelasticity of highly vibrationally excited NO on Ag(111). *J. Phys. Chem. Lett.* **2016**, *7*, 441−446.

(13) Werdecker, J.; Shirhatti, P. R.; Golibrzuch, K.; Bartels, C.; Wodtke, A. M.; Harding, D. J. Electronically nonadiabatic vibrational excitation of N_2 scattered from Pt(111). *J. Phys. Chem. C* **2015**, *119*, 14722−14727.

(14) Geweke, J.; Shirhatti, P. R.; Rahinov, I.; Bartels, C.; Wodtke, A. M. Vibrational energy transfer near a dissociative adsorption transition state: State-to-state study of HCl collisions at Au(111). *J. Chem. Phys.* **2016**, *145*, 054709.

(15) Schäfer, T.; Bartels, N.; Golibrzuch, K.; Bartels, C.; Köckert, H.; Auerbach, D. J.; Kitsopoulos, T. N.; Wodtke, A. M. Observation of direct vibrational excitation in gas-surface collisions of CO with Au(111): a new model system for surface dynamics. *Phys. Chem. Chem. Phys.* **2013**, *15*, 1863−1867.

(16) Kroes, G. J.; Díaz, C.; Pijper, E.; Olsen, R. A.; Auerbach, D. J. Apparent failure of the Born-Oppenheimer static surface model for vibrational excitation of molecular hydrogen on copper. *Proc. Natl. Acad. Sci. U. S. A.* **2010**, *107*, 20881−20886.

(17) Kroes, G. J.; Wiesenekker, G.; Baerends, E. J.; Mowrey, R. C. Competition between vibrational excitation and dissociation in collisions of H_2 with Cu(100). *Phys. Rev. B: Condens. Matter Mater. Phys.* **1996**, *53*, 10397−10401.

(18) McCormack, D. A.; Kroes, G. J.; Olsen, R. A.; Baerends, E. J.; Mowrey, R. C. Rotational effects on vibrational excitation of H_2 on Cu(100). *Phys. Rev. Lett.* **1999**, *82*, 1410−1413.

(19) Díaz, C.; Pijper, E.; Olsen, R. A.; Busnengo, H. F.; Auerbach, D. J.; Kroes, G. J. Chemically accurate simulation of a prototypical surface reaction: H_2 dissociation on Cu(111). *Science* **2009**, *326*, 832−834.

(20) Nattino, F.; Genova, A.; Guijt, M.; Muzas, A. S.; Díaz, C.; Auerbach, D. J.; Kroes, G. J. Dissociation and recombination of D_2 on Cu(111): Ab initio molecular dynamics calculations and improved analysis of desorption experiments. *J. Chem. Phys.* **2014**, *141*, 124705.

(21) Nattino, F.; Díaz, C.; Jackson, B.; Kroes, G. J. Effect of surface motion on the rotational quadrupole alignment parameter of D_2 reacting on Cu(111). *Phys. Rev. Lett.* **2012**, *108*, 236104.

(22) Díaz, C.; Olsen, R. A.; Auerbach, D. J.; Kroes, G. J. Six dimensional dynamics study of reactive and non reactive scattering of H_2 from Cu(111) using a chemically accurate potential energy surface. *Phys. Chem. Chem. Phys.* **2010**, *12*, 6499−6519.

(23) Kroes, G. J.; Pijper, E.; Salin, A. Dissociative chemisorption of H_2 on the Cu(110) surface: A quantum and quasiclassical dynamical study. *J. Chem. Phys.* **2007**, *127*, 164722.

(24) Blanco-Rey, M.; Juaristi, J. I.; Díez Muiño, R.; Busnengo, H. F.; Kroes, G. J.; Alducin, M. Electronic friction dominates hydrogen hot-atom relaxation on Pd(100). *Phys. Rev. Lett.* **2014**, *112*, 103203.

(25) Saalfrank, P.; Juaristi, J. I.; Alducin, M.; Blanco-Rey, M.; Díez Muiño, R. Vibrational lifetimes of hydrogen on lead films: An ab initio molecular dynamics with electronic friction (AIMDEF) study. *J. Chem. Phys.* **2014**, *141*, 234702.

(26) Novko, D.; Blanco-Rey, M.; Alducin, M.; Juaristi, J. I. Surface electron density models for accurate ab initio molecular dynamics with electronic friction. *Phys. Rev. B: Condens. Matter Mater. Phys.* **2016**, *93*, 245435.

(27) Novko, D.; Blanco-Rey, M.; Juaristi, J. I.; Alducin, M. Ab initio molecular dynamics with simultaneous electron and phonon excitations: Application to the relaxation of hot atoms and molecules on metal surfaces. *Phys. Rev. B: Condens. Matter Mater. Phys.* **2015**, *92*, 201411.

(28) Martin-Gondre, L.; Alducin, M.; Bocan, G. A.; Díez Muiño, R.; Juaristi, J. I. Competition between electron and phonon excitations in the scattering of nitrogen atoms and molecules off tungsten and silver metal surfaces. *Phys. Rev. Lett.* **2012**, *108*, 096101.

(29) Galparsoro, O.; Pétuya, R.; Juaristi, J. I.; Crespos, C.; Alducin, M.; Larrégaray, P. Energy dissipation to tungsten surfaces upon Eley-Rideal recombination of N_2 and H_2. *J. Phys. Chem. C* **2015**, *119*, 15434−15442.

DOI: 10.1021/acs.jpcc.7b01096
J. Phys. Chem. C 2017, 121, 13617−13633

(30) Karplus, M.; Porter, R. N.; Sharma, R. D. Exchange reactions with activation energy. I. Simple barrier potential for (H,H_2). *J. Chem. Phys.* **1965**, *43*, 3259−3287.
(31) Adelman, S. A.; Doll, J. D. Generalized Langevin equation approach for atom/solidsurface scattering: General formulation for classical scattering off harmonic solids. *J. Chem. Phys.* **1976**, *64*, 2375−2388.
(32) Tully, J. C. Dynamics of gas-surface interactions: 3D generalized Langevin model applied to fcc and bcc surfaces. *J. Chem. Phys.* **1980**, *73*, 1975−1985.
(33) Busnengo, H. F.; Di Césare, M. A.; Dong, W.; Salin, A. Surface temperature effects in dynamic trapping mediated adsorption of light molecules on metal surfaces: H_2 on Pd(111) and Pd(110). *Phys. Rev. B: Condens. Matter Mater. Phys.* **2005**, *72*, 125411.
(34) Lončarić, I.; Alducin, M.; Saalfrank, P.; Juaristi, J. I. Femtosecond-laser-driven molecular dynamics on surfaces: Photodesorption of molecular oxygen from Ag(110). *Phys. Rev. B: Condens. Matter Mater. Phys.* **2016**, *93*, 014301.
(35) Head-Gordon, M.; Tully, J. C. Molecular dynamics with electronic frictions. *J. Chem. Phys.* **1995**, *103*, 10137−10145.
(36) Juaristi, J. I.; Alducin, M.; Díez Muiño, R.; Busnengo, H. F.; Salin, A. Role of electron-hole pair excitations in the dissociative adsorption of diatomic molecules on metal surfaces. *Phys. Rev. Lett.* **2008**, *100*, 116102.
(37) Echenique, P. M.; Nieminen, R. M.; Ritchie, R. H. Density functional calculation of stopping power of an electron gas for slow ions. *Solid State Commun.* **1981**, *37*, 779−781.
(38) Echenique, P. M.; Nieminen, R. M.; Ashley, J. C.; Ritchie, R. H. Nonlinear stopping power of an electron gas for dlow ions. *Phys. Rev. A: At., Mol., Opt. Phys.* **1986**, *33*, 897−904.
(39) Winter, H.; Juaristi, J. I.; Nagy, I.; Arnau, A.; Echenique, P. M. Energy loss of slow ions in a nonuniform electron gas. *Phys. Rev. B: Condens. Matter Mater. Phys.* **2003**, *67*, 245401.
(40) Juaristi, J. I.; Arnau, A.; Echenique, P. M.; Auth, C.; Winter, H. Charge state dependence of the energy loss of slow ions in metals. *Phys. Rev. Lett.* **1999**, *82*, 1048−1051.
(41) Bünermann, O.; Jiang, H. Y.; Dorenkamp, Y.; Kandratsenka, A.; Janke, S. M.; Auerbach, D. J.; Wodtke, A. M. Electron-hole pair excitation determines the mechanism of hydrogen atom adsorption. *Science* **2015**, *350*, 1346−1349.
(42) Goikoetxea, I.; Juaristi, J. I.; Alducin, M.; Diéz Muiño, R. Dissipative effects in the dynamics of N_2 on tungsten surfaces. *J. Phys.: Condens. Matter* **2009**, *21*, 264007.
(43) Füchsel, G.; Schimka, S.; Saalfrank, P. On the role of electronic friction for dissociative adsorption and scattering of hydrogen molecules at a Ru(0001) surface. *J. Phys. Chem. A* **2013**, *117*, 8761−8769.
(44) Muzas, A. S.; Juaristi, J. I.; Alducin, M.; Díez Muiño, R.; Kroes, G. J.; Díaz, C. Vibrational deexcitation and rotational excitation of H_2 and D_2 scattered from Cu(111): Adiabatic versus non-adiabatic dynamics. *J. Chem. Phys.* **2012**, *137*, 064707.
(45) Springer, C.; Head-Gordon, M.; Tully, J. C. Simulations of femtosecond laser-induced desorption of CO from Cu(100). *Surf. Sci.* **1994**, *320*, L57−L62.
(46) Hammer, B.; Hansen, L. B.; Nørskov, J. K. Improved adsorption energetics within density-functional theory using revised Perdew-Burke-Ernzerhof functionals. *Phys. Rev. B: Condens. Matter Mater. Phys.* **1999**, *59*, 7413−7421.
(47) Perdew, J. P.; Chevary, J. A.; Vosko, S. H.; Jackson, K. A.; Pederson, M. R.; Singh, D. J.; Fiolhais, C. Atoms, molecules, solids, and surfaces: applications of the generalized gradient approximation for exchange and correlation. *Phys. Rev. B: Condens. Matter Mater. Phys.* **1992**, *46*, 6671−6687.
(48) Perdew, J. P.; Burke, K.; Ernzerhof, M. Generalized gradient approximation made simple. *Phys. Rev. Lett.* **1996**, *77*, 3865−3868.
(49) Füchsel, G.; del Cueto, M.; Díaz, C.; Kroes, G. J. Enigmatic HCl + Au(111) reaction: a puzzle for theory and experiment. *J. Phys. Chem. C* **2016**, *120*, 25760−25779.
(50) Marston, C. C.; Balint-Kurti, G. G. The Fourier grid Hamiltonian method for bound state eigenvalues and eigenfunctions. *J. Chem. Phys.* **1989**, *91*, 3571−3576.
(51) Kroeger, F. R.; Swenson, C. A. Absolute linear thermal-expansion measurements on copper and aluminum from 5 to 320 K. *J. Appl. Phys.* **1977**, *48*, 853−864.
(52) Leksina, I. E.; Novikova, S. I. Thermal expansion of copper, silver, and gold within a wide range of temperatures. *Sov. Phys.—Solid State* **1963**, *5*, 798−801.
(53) Beeman, D. Some multistep methods for use in molecular-dynamics calculations. *J. Comput. Phys.* **1976**, *20*, 130−139.
(54) Tully, J. C.; Gilmer, G. H.; Shugard, M. Molecular dynamics of surface diffusion. 1. Motion of adatoms and clusters. *J. Chem. Phys.* **1979**, *71*, 1630−1642.
(55) Kresse, G.; Furthmüller, J. Efficient iterative schemes for ab initio total-energy calculations using a plane-wave basis set. *Phys. Rev. B: Condens. Matter Mater. Phys.* **1996**, *54*, 11169−11186.
(56) Kresse, G.; Hafner, J. Norm-conserving and ultrasoft pseudopotentials for first-row and transition elements. *J. Phys.: Condens. Matter* **1994**, *6*, 8245−8257.
(57) Vanderbilt, D. Soft self-consistent pseudopotentials in a generalized eigenvalue formalism. *Phys. Rev. B: Condens. Matter Mater. Phys.* **1990**, *41*, 7892−7895.
(58) Wang, Z. S.; Darling, G. R.; Holloway, S. Surface temperature dependence of the inelastic scattering of hydrogen molecules from metal surfaces. *Phys. Rev. Lett.* **2001**, *87*, 226102.
(59) Hirshfeld, F. L. Bonded-atom fragments for describing molecular charge-densities. *Theoret.Chim.Acta* **1977**, *44*, 129−138.
(60) Rittmeyer, S. P.; Meyer, J.; Juaristi, J. I.; Reuter, K. Electronic friction-based vibrational lifetimes of molecular adsorbates: Beyond the independent-atom approximation. *Phys. Rev. Lett.* **2015**, *115*, 046102.
(61) Puska, M. J.; Nieminen, R. M. Atoms embedded in an electron-gas - phase-shifts and cross-sections. *Phys. Rev. B: Condens. Matter Mater. Phys.* **1983**, *27*, 6121−6128.
(62) Murphy, M. J.; Hodgson, A. Adsorption and desorption dynamics of H_2 and D_2 on Cu(111): The role of surface temperature and evidence for corrugation of the dissociation barrier. *J. Chem. Phys.* **1998**, *108*, 4199−4211.
(63) Michelsen, H. A.; Rettner, C. T.; Auerbach, D. J. On the influence of surface-temperature on adsorption and desorption in the D_2/Cu(111) system. *Surf. Sci.* **1992**, *272*, 65−72.
(64) Michelsen, H. A.; Rettner, C. T.; Auerbach, D. J.; Zare, R. N. Effect of rotation on the translational and vibrational energy dependence of the dissociative adsorption of D_2 on Cu(111). *J. Chem. Phys.* **1993**, *98*, 8294−8307.
(65) Kosloff, R. Time-dependent quantum-mechanical methods for molecular dynamics. *J. Phys. Chem.* **1988**, *92*, 2087−2100.
(66) Pijper, E.; Kroes, G. J.; Olsen, R. A.; Baerends, E. J. Reactive and diffractive scattering of H_2 from Pt(111) studied using a six-dimensional wave packet method. *J. Chem. Phys.* **2002**, *117*, 5885−5898.
(67) Bonnet, L. Classical dynamics of chemical reactions in a quantum spirit. *Int. Rev. Phys. Chem.* **2013**, *32*, 171−228.
(68) Saalfrank, P. Quantum dynamical approach to ultrafast molecular desorption from surfaces. *Chem. Rev.* **2006**, *106*, 4116−4159.
(69) Monturet, S.; Saalfrank, P. Role of electronic friction during the scattering of vibrationally excited nitric oxide molecules from Au(111). *Phys. Rev. B: Condens. Matter Mater. Phys.* **2010**, *82*, 075404.
(70) Füchsel, G.; Tremblay, J. C.; Klamroth, T.; Saalfrank, P. Selective excitation of molecule-surface vibrations in H_2 and D_2 dissociatively adsorbed on Ru(0001). *Isr. J. Chem.* **2012**, *52*, 438−451.
(71) Gelman, D.; Kosloff, R. Simulating dissipative phenomena with a random phase terminal wave functions, high temperature application of the Surrogate Hamiltonian approach. *Chem. Phys. Lett.* **2003**, *381*, 129−138.
(72) Nest, M.; Kosloff, R. Quantum dynamical treatment of inelastic scattering of atoms at a surface at finite temperature: The random

DOI: 10.1021/acs.jpcc.7b01096
J. Phys. Chem. C 2017, 121, 13617−13633

phase thermal wave function approach. *J. Chem. Phys.* **2007**, *127*, 134711.
(73) Lüder, F.; Nest, M.; Saalfrank, P. Temperature effects for vibrational relaxation of hydrogen adsorbed on Si(100): a stochastic multiconfigurational time-dependent Hartree (MCTDH) study. *Theor. Chem. Acc.* **2010**, *127*, 183−193.
(74) Lorenz, U.; Saalfrank, P. Comparing thermal wave function methods for multi-configuration time-dependent Hartree simulations. *J. Chem. Phys.* **2014**, *140*, 044106.
(75) Qu, C.; Bowman, J. M. Revisiting adiabatic switching for initial conditions in quasi-classical trajectory calculations: Application to CH_4. *J. Phys. Chem. A* **2016**, *120*, 4988−4993.
(76) Dion, M.; Rydberg, H.; Schröder, E.; Langreth, D. C.; Lundqvist, B. I. Van der Waals density functional for general geometries. *Phys. Rev. Lett.* **2004**, *92*, 246401.
(77) Lee, K.; Murray, E. D.; Kong, L. Z.; Lundqvist, B. I.; Langreth, D. C. Higher-accuracy van der Waals density functional. *Phys. Rev. B: Condens. Matter Mater. Phys.* **2010**, *82*, 081101R.
(78) Berland, K.; Cooper, V. R.; Lee, K.; Schröder, E.; Thonhauser, T.; Hyldgaard, P.; Lundqvist, B. I. van der Waals forces in density functional theory: a review of the vdW-DF method. *Rep. Prog. Phys.* **2015**, *78*, 066501.
(79) Hyldgaard, P.; Berland, K.; Schröder, E. Interpretation of van der Waals density functionals. *Phys. Rev. B: Condens. Matter Mater. Phys.* **2014**, *90*, 075148.
(80) Nattino, F.; Migliorini, D.; Kroes, G. J.; Dombrowski, E.; High, E. A.; Killelea, D. R.; Utz, A. L. Chemically accurate simulation of a polyatomic molecule-metal surface reaction. *J. Phys. Chem. Lett.* **2016**, *7*, 2402−2406.
(81) Wijzenbroek, M.; Klein, D. M.; Smits, B.; Somers, M. F.; Kroes, G. J. Performance of non-local van der Waals density functional on the dissociation of H_2 on metal surfaces. *J. Phys. Chem. A* **2015**, *119*, 12146−12158.
(82) Andersson, S.; Persson, M. Sticking in the physisorption well: Influence of surface structure. *Phys. Rev. Lett.* **1993**, *70*, 202−205.
(83) Andersson, S.; Persson, M. Crystal-face dependence of physisorption potentials. *Phys. Rev. B: Condens. Matter Mater. Phys.* **1993**, *48*, 5685−5688.
(84) Lee, K.; Kelkkanen, A. K.; Berland, K.; Andersson, S.; Langreth, D. C.; Schröder, E.; Lundqvist, B. I.; Hyldgaard, P. Evaluation of a density functional with account of van der Waals forces using experimental data of H_2 physisorption on Cu(111). *Phys. Rev. B: Condens. Matter Mater. Phys.* **2011**, *84*, 193408.
(85) Lee, K.; Berland, K.; Yoon, M.; Andersson, S.; Schröder, E.; Hyldgaard, P.; Lundqvist, B. I. Benchmarking van der Waals density functionals with experimental data: potential-energy curves for H_2 molecules on Cu(111), (100), and (110) surfaces. *J. Phys.: Condens. Matter* **2012**, *24*, 424213.
(86) Klimeš, J.; Bowler, D. R.; Michaelides, A. Chemical accuracy for the van der Waals density functional. *J. Phys.: Condens. Matter* **2010**, *22*, 022201.
(87) Luntz, A. C.; Persson, M.; Sitz, G. O. Theoretical evidence for nonadiabatic vibrational deexcitation in $H_2(D_2)$ state-to-state scattering from Cu(100). *J. Chem. Phys.* **2006**, *124*, 091101.
(88) Askerka, M.; Maurer, R. J.; Batista, V. S.; Tully, J. C. Role of tensorial friction in energy transfer at metal surfaces. *Phys. Rev. Lett.* **2016**, *116*, 217601.
(89) Novko, D.; Alducin, M.; Blanco-Rey, M.; Juaristi, J. I. Effects of electronic relaxation processes on vibrational linewidths of adsorbates on surfaces: The case of CO/Cu(100). *Phys. Rev. B: Condens. Matter Mater. Phys.* **2016**, *94*, 224306.

DOI: 10.1021/acs.jpcc.7b01096
J. Phys. Chem. C 2017, 121, 13617−13633